MOLECULAR MECHANISM OF *FAT* SIGNALING PATHWAY COORDINATING GROWTH AND PATTERNING IN *DROSOPHILA MELANOGASTER*

by

GUOHUI PAN

A dissertation submitted to the

Graduate School-New Brunswick

Rutgers, The State University of New Jersey

and

The Graduate School of Biomedical Sciences

University of Medicine and Dentistry of New Jersey

In partial fulfillment of the requirements

For the degree of

Doctor of Philosophy

Graduate Program in Neuroscience

Written under the direction of

Kenneth D. Irvine

And approved by

_____

_____

_____

_____

New Brunswick, New Jersey

MAY, 2013

ABSTRACT OF THE DISSERTATION

MOLECULAR MECHANISM OF *FAT* SIGNALING PATHWAY COORDINATING GROWTH AND PATTERNING IN *DROSOPHILA MELANOGASTER*

By GUOHUI PAN

Dissertation Director:

Kenneth D. Irvine

From an RNAi lines screen, our lab found the *Drosophila* Zyxin family gene, *Zyx102* (Zyx) as a negative regulator of Fat-Hippo signaling. Epistasis analysis put Zyx between Dachs and Warts (Wts) in the Fat-branch, and Zyx-RNAi suppresses the reduction of Wts level by fat RNAi. Zyx partially co-localizes with Dachs, and its localization was not altered by manipulating other Fat-branch component. Zyx protein binds to Dachs, and Dachs stimulates binding of Zyx to Wts, suggesting a molecular mechanism for how Fat signaling regulates Wts through Dachs. Our results identified a new component of Fat signaling, and investigated possible molecular mechanism for signal transduction from Fat to Wts.

Among the vast amount of genes involved in organ morphogenesis, Fat gene stands out as it transduces both growth cue and planar cell polarity (PCP). But the molecular mechanism underlying is unknown. A structure-function approach is recruited to figure out the motifs in Fat that are required for signal transduction mechanism.

By a fat genomic Bac Clone, which is expressed under endogenous condition, activities that could be missed by over-expression can be revealed. We find out the PCP activity is evolutionarily conserved from Drosophila to mammals. And the Hippo and PCP activity can be largely separated at the level of the Fat receptor. A specific motif was identified to mainly impair Fat-Hippo activity and reduce Fat phosphorylation. Manipulating the potential phosphorylation sites in this motif gives similar phenotypes, implicating phosphorylation as an essential factor in Fat-Hippo signal transduction. This motif overlaps with the previously identified Dco binding site, but retains normal binding affinity.

Another conserved four amino acid motif is crucial for Fat-PCP, while the Fat-Hippo activity is almost normal. And this motif contributes differently to multiple PCP assays, suggesting there are different kinds of PCP in *Drosophila*.

Different Fat activity leads to distinctive Dachs localization pattern, and directly manipulating Dachs localization could phenocopy loss of Fat activity. Thus Dachs localization influences both Hippo and PCP phenotypes.

Our results identify a conserved mechanism of Fat signaling, establish functional significances for Fat ICD motif, phosphorylation sites, and Dachs membrane localization to downstream pathways.

Acknowledgement

Pursuing a Ph.D. degree has been an overwhelming experience for me. The real learning experience, the academic topic I have been working on, team work, how to write papers and proposals, give talks, science meeting and networking…compose the precious journey to the final achievement. In any case, I am indebted to many people for making the time working on my Ph.D. an unforgettable career.

First of all, I am deeply grateful to my advisor Kenneth D. Irvine, for his support, advising, training, insights, patience, and tolerance. You have been a steady influence throughout my Ph.D. career; you have oriented and supported me with promptness and care, and have always been patient and encouraging in times of difficulties; your ability to select and to approach compelling research problems, your high scientific standards, and your hard work set an example; your generosity and comprehension in assisting my personal pursuit. All these are the best I ever got in the past five years, which I appreciate from my heart.

Furthermore, I am very grateful to my committee Richard Padgett, Ruth Steward, Michael Matise, for insight comments both in my work and in this thesis, for many motivating discussions and help.

In addition, I have been very privileged to get know and to collaborate with many other great people who I worked with over the last several years. I learned a lot from you about life, research, how to tackle new problems and how to develop techniques to solve them. Cordelia Rauskolb has been a great teacher and co-author. Your technical excellence and tremendous experimental experience provided great help to my research. And I also enjoy your fine cooking. I worked with Yongqiang Feng for less than two years before

his graduation, and he patiently taught me experimental techniques, and generously provided lots of data and hints to follow up. Collaboration with Abhijit A. Ambegaonkar and Gongping Sun has been a wonderful team work, we benefit a lot from each other, and expedite research progress. It would be impossible for me to go smoothly with my project without the assistance, training, and valuable comments from former and current lab members, in particular, B.V.Venugopala Reddy (Venu), Hyangyee Oh, Maoyao Pan, Aiguo Xu, Hiroyuki O. Ishikawa, Binnaz Kucuk, Shemeeakah Powell, Kanchan Puttaswamy, Xunlei Kang, Elmira Kirichenko, Tricia Graham, Veronica Codelia, Luna Ballesteros, Shuguo Sun, Yuanwang Pan. I would like to thank the student I had the pleasure to work with. Matthew Huff and Tahia Haque assist me in this project.

I am very grateful to the Program of Neuroscience, for giving me the opportunity to join Rutgers University, for the flexibility of choosing research fields, for the care and help from John Pintar and Joan Mordes.

The work on this thesis was supported by Howard Hughes Medical Institute and the NIH. The Developmental Studies Hybridoma Bank and the Bloomington stock center for plasmids, antibodies and *Drosophila* stocks. The Graduate Program of Neuroscience provided the first year graduate fellowship.

Finally, I am indebted to my mom, dad, and my love for their infinite support and sacrifice throughout everything.

TABLE OF CONTENTS

LIST OF ILLUSTRATIONS

CHAPTER I

General Introduction

Drosophila imaginal discs as a model system to study organ development

How the growth and patterning of tissue development are controlled and coordinated has been one of the fundamental questions in developmental biology. One classic model system for the study of growth regulation is the wing imaginal disc of *Drosophila melanogaster* (fruit fly) [1], due to its relative simplicity and the availability of various genetic and biochemical tools. Imaginal discs are a single epithelial layer, responsible for the characteristic surface patterning of *Drosophila melanogaster*. They arise and become determined (wingness, legness) during embryogenesis [2], proliferate during the larval instars, giving the adult appendages and other cuticular structures, such as leg, wing, head etc. at metamorphosis [3]. Most of the studies in this dissertation focus on the wing imaginal discs.

Hippo pathway regulating growth

Hippo signaling, also known as the Salvador-Warts-Hippo pathway, has emerged as an important pathway involved in tissue growth regulation, cell-fate determination, mitosis, various cancers, stem cell proliferation and differentiation, pluripotency [4-7]. Many components of the Hippo pathway were identified as a result of mutations in *Drosophila melanogaster* that resulted in tissue overgrowth [7]. The pathway is conserved in vertebrates, including mammals, in which changing the activity of Hippo signaling also results in dramatic changes in certain organ sizes [8, 9]. Abnormal Hippo pathway activity has been reported in many human cancers [7]. For example, the human homolog

of *Drosophila melanogaster* Merlin is a bona fide tumor suppressor involved in human tumorigenesis [10].

The center of Hippo pathway is the Hippo kinase cassette, which comprises the tumor suppressors Hpo, Wts, Salvador (Sav) and Mob-as tumor suppressor (Mats). When activated, Hpo undergoes autophosphorylation [11, 12], and then phosphorylates Wts, Sav, and Mats [13, 14]. Sav facilitates Wts phosphorylation by Hpo, and serves as scaffolding protein between Hpo and Wts [14]. Phosphorylation by Hpo promotes Mats-Wts binding, and Mats is required as a co-factor for Wts activity [13, 15]. Wts also undergoes autophosphorylation [13]. Normally this Hpo-Wts cassette regulates Wts activity by controlling its phosphorylation (Figure 1). When phosphorylated, Wts could phosphorylate the transcriptional co-activator Yorkie (Yki, Yap and Taz in vertebrate), and retain Yki in cytoplasm, thus preventing Yki from entering nucleus and activating downstream growth-promoting genes and apoptosis inhibitors, such as DIAP1, cyclin E, and bantam microRNA [1, 16, 17].

Recent years, multiple pathways have been discovered to impinge into Hippo pathway [7, 18]. The FERM domain proteins Merlin and Expanded (Ex) has long been identified to represent two different upstream braches, and recently the WW domain protein Kibra was found to act in the Merlin branch [19]. Many Hippo pathway components reside at cell junctions, some junction proteins are found to regulate Hippo signaling, such as the adherens junction protein Ajuba (Jub) and the apical-basal polarity proteins Discs large (Dlg), Lethal giant larvae (Lgl), Scribble (Scrib), Crumbs, and atypical protein kinase C (aPKC) [7]. For example, the transmembrane protein Crumbs binds to Ex and activates Hippo signaling. Hippo pathway is also regulated by Jun kinase (JNK) during

regeneration [20]. Another major input, the Fat/Dachsous (Ds) signaling, is thought to impinge on the Hpo-Wts cassette by affecting the protein level of Wts, through Discs overgrown (Dco), Dachs, Lowfat (lft), and Zyx [21], which will be described below.

Planar Cell Polarity (PCP)

Cell polarization is essential for the correct anatomy and function of tissues. In addition to exhibiting apical-basal polarity, epithelial cells possess a second type of polarity, known as planar polarity, which runs perpendicular to the apical-basal axis [22]. Studies in *Xenopus*, mouse, zebrafish, and chick have revealed the essential role of planar polarity in regulating multiple aspects of vertebrate development [23]. And mutations in key planar polarity genes or downstream effectors contribute to various human diseases, such as birth defect and cancers [24]. The genetic control of planar polarity is highly conserved between flies and vertebrates. In fruit flies, polarity can be easily observed in pupal and adult wings by the presence of small wing hairs (trichomes), which form at about 32 hour after pupa formation from the distal side of each cell [22, 25]. Cuticle ridges also requires planar polarity, which run along the anterior-posterior axis in the anterior of the wing and along the proximal-distal axis in the posterior of the wing [26]. Losing planar polarity cues in these tissue results in a swirl-like pattern of wing hair and mis-orientation in ridges. Genetic studies have figured out two major groups of PCP regulating system: Fz-dependent (also known as core system), and the Fat/Ds-dependent system [23]. The core system plays a central role in PCP and recruits Frizzled (Fz), Dishevelled (Dsh), Diego (Dgo), Strabismus (Stbm), Prickle (Pk), Flamingo (Fmi). Fat/Ds system emerges as an alternative regulating pathway for PCP, besides its role in regulating tissue growth through Hippo signaling (descripted below). In *fat*, *ds*, or *dachs*

mutants, the orientation of cell division is randomized, rendering the wings to be rounder than normal [27, 28]. The relationship between core system and Fat/Ds system in regulating PCP is not clear. And the dual roles of Fat signaling in growth control and PCP implicates potential coordination of pattern control with tissue growth.

Fat-Hippo and Fat-PCP signaling

Fat is a large atypical cadherin protein serving as a transmembrane receptor for signal transduction pathways that regulate growth (Hippo signaling) and PCP [5, 22, 29]. *Drosophila fat* is the first gene identified in the Fat subfamily, in 1991 [30]. The Fat subfamily of cadherins is conserved from flies to mammals. There are four Fat genes (Fat1-Fat4) in mammalian and two in *Drosophila* (Fat and Kugelei/Fat-like/*Drosophila* Fat2). They commonly have 34 cadherin repeats, one or two laminin A-G domains and several epidermal growth factor (EGF) motifs in their extracellular regions [30]. Sequence comparison suggested that Fat4 shows modest sequence similarity to *Drosophila* Fat, while mammalian Fat1, Fat2, Fat3 and Kugelei fall into another subfamily. Their huge molecular masses (about 500-600 kDa) have hindered studies of the molecular aspects of their roles. Recent studies show that mammalian Fat4 is an essential gene that has a key role in vertebrate PCP [31]. Loss of Fat4 leads to defects in elongation of the cochlea, orientation of hair cells in the inner ear, and neural tube elongation [32]. Fat4 represses expression of *four-jouinted X1(Fjx1)*, the sole vertebrate homolog of *Drosophila fj*, suggesting the Fat4-PCP signal pathway is conserved from that of *Drosophila* [31].

Drosophila Fat is regulated by two proteins expressed in gradients: Dachsous (Ds) and Four-jointed (Fj). Ds also encodes an atypical cadherin that can function as a ligand for

Fat [5]. Fj is a golgi-localized kinase that phosphorylates cadherin domains of Fat and Ds to modulate binding between them [33-35]. Rather than responding solely to the level of Ds and Fj, Fat is also regulated by the slope and vector of their expression gradients, with the slope influencing Hippo signaling and the vector influencing PCP [22, 36, 37].

The Fat-Hippo pathway exerts activity through affecting Wts level [21]. The molecular mechanism by which Fat-Hippo signaling being transduced to influences the level of Wts protein is not well understood, but several genes have been identified as playing key roles in Fat signal transduction: *dachs*, *dc*), *Jub* and *Zyx*. Mutation of *fat* or *dco* reduces Wts protein levels and causes overgrowth, which could be suppressed by overexpression of Wts. Overexpression of Dachs, or knocking-down Zyx by RNAi, suppresses the Wts reduction by *fat* mutations. This effect is post-transcriptional because Wts expressed from a heterologous promoter could also be affected. However, there are still a lot of gaps in Fat signaling pathway.

Fat regulating Dachs localization

Dachs is genetically required for the influence of Fat on Wts levels, downstream gene expression, and organ growth [21, 38]. Fat regulates the localization of Dachs to the sub-apical membrane: when *fat* is mutant, Dachs accumulates on the membrane around the entire circumference of the cell, and when Fat is overexpressed, Dachs is mostly cytoplasmic [38]. In imaginal discs and optic neuroepithelia, Dachs membrane localization is polarized within the plane of the tissue, in response to the graded expression of Ds and Fj [34, 36, 38-40]. The correlation of Dachs localization with Fat activity implicates Dachs regulation as a key step in Fat signaling, but how it transduces Fat-Hippo and Fat-PCP signaling differentially is unknown. It has been proposed that the

influence of Dachs on Fat-Hippo signaling is related to the amount of Dachs localized to the membrane, whereas its influence on PCP is related to the direction in which Dachs membrane localization is polarized [29, 36]. Some studies proposes that Dachs myosin motor activity may contribute to the orientation of wing cell division by contracting cell apices, thereby altering cell geometry [28]. Modulation of tension along intercellular junctions also appears to contribute to influences of Dachs on PCP in the notum [40].

Dco regulating phosphorylation of Fat intracellular domain

dco mutant leads to overgrowth in mosaic clones, and is identified as *Drosophila* Casein kinase I ε [41], which has been implicated in a variety of pathways including Wnt and Hedgehog signaling [42]. Besides its role in growth regulation, it was also implied in the PCP regulation through Fz-dependent pathway [43, 44] and cell viability control by post-transcriptionally regulating caspase inhibitor DIAP1 level [45]. However, the complexity of Dco mal-function phenotype renders it difficult to interpret. Two point mutations at the conserved domains of Dco lead to an antimorphic allele, dco^{3}, which specific impairs Fat-Hippo signaling, but not Fat-PCP signaling [21, 46]. Dco is also required for the phosphorylation of Fat intracellular domain (ICD), suggesting Fat ICD phosphorylation is a key step in Fat-Hippo signal transduction [46, 47].

***Zyxin* and *Jub* as new player in Fat signaling**

Recently, two new components of Fat-Hippo signaling have been characterized—the 3-LIM domain proteins Zyx and Jub. From LIM domain and other motif comparisons, Zyx may represent the paralogous class Lipoma preferred partner (LPP), Zyxin, and Thyroid-receptor interacting protein 6 (TRIP6), while Jub may represent Ajuba, LIM Domains Containing 1 (LIMD1) and Wilms tumor protein 1 interacting protein (WTIP) [48, 49].

These 3-LIM domain family members feature three carboxy-terminal LIM domains, proline-rich motifs, and potential nuclear export signals in the amino-terminal two-thirds of the protein [49]. Zyxin/Ajuba family proteins have been reported to be involved in maintaining cell structure, cell fate, and differentiation [50]. Zyxin is a regulator of actin filament assembly, and proper localization of Zyxin to focal adhesions is necessary for the accumulation of ENA/VASP proteins to these sites [50, 51]. Zyxin and Ajuba could shuttle between sites of focal adhesions/cell-cell contacts and the nucleus [52-54]. Although the exact reason for cycling is not known, it has been speculated to involve transducing signals from the sites of attachment to the nucleus [55]. During mitosis, Zyxin is targeted to mitotic apparatus, and interacts with mitotic regulators Lats1 [56, 57]. LIMD1 is also phosphorylated during mitosis [55]. Zyxin could also transit to nucleus in response to mechanical stimuli, and is required for mechanosensitive gene expression [58]. Ajuba functions as nuclear receptor co-repressor and negatively regulates retinoic acid signaling [59].

The *Drosophila* Jub is reported to serve as a negative regulator of Hippo pathway activity [48]. The epistasis analysis suggests that Jub acts upstream of Wts and Yki but downstream of Hpo. And Jub/Ajuba binds to Wts/LATS1/LATS2 and Sav/WW45, but not Hpo/Mst1. More intriguingly, human LIMD1 (most closely related to Jub) suppress the phospho-Yap level induced by MST1, WW45, and LATS1/2. Meanwhile, our lab discovered Zyx as a new Fat-hippo component, between Dachs and Wts in the Fat-branch [60]. Zyxin and Dachs can bind each other, and binding of Dachs to Zyxin could stimulate Zyxin-Wts binding [60]. Similarly, In mammalian cells, Zyxin binds to LATS1 during mitosis or after Cdc2 promoted phosphorylation [56].

Summary of significant progresses in the thesis research

Zyxin Links Fat Signaling to the Hippo Pathway

To improve understanding of the Fat-Hippo signaling pathway, we conducted an RNAi lines screen to identify additional pathway components. We identified *Zyx* (*Drosophila Zyx102*) as an essential component of Fat-Hippo signaling. Depletion of Zyx in *Drosophila* wing discs using RNAi decreases the wing size, down-regulates Hippo signaling targets ex-laZ, th-laZ, and DIAP1. Epistasis analysis put Zyx between Dachs and Wts in the Fat-branch: Zyx-Wts double RNAi displays a phenotype identical to Wts-RNAi. Zyx-RNAi could suppress the overgrowth phenotype caused by Fat-RNAi, Dco^3, and overexpression of Dachs. And biochemically, Zyx-RNAi suppresses the reduction of Wts level by fat RNAi. Zyx partially co-localizes with Dachs. And unlike Dachs, its localization was not altered by manipulating other Fat-branch component: neither does manipulating Zyx affect Dachs localization. Thus Zyx exerts its function by regulating Wts protein level in vivo. Zyx protein binds to Dachs, and Dachs stimulates binding of Zyx to Wts, suggesting a molecular mechanism for how Fat signaling regulates Wts through Wts. Our results identified a new component of Fat signaling, investigated its genetic relationship with other Fat pathway components, and proposed possible molecular mechanism for signal transduction from Fat to Wts.

Separating different Fat activities on molecular level

The large atypical cadherin Fat is a receptor for both Hippo and planar cell polarity (PCP) pathways. Here we investigate the molecular basis for signal transduction downstream of Fat by creating targeted alterations within a genomic construct that contains the entire *fat* locus. Targeted deletion of conserved motifs identifies a four amino acid C-terminal

motif (FatΔF) that is essential for aspects of Fat-mediated PCP, meanwhile, another internal motif (FatΔD) that contributes mainly to Fat-Hippo signaling. Thus, the Fat-Hippo and Fat-PCP activities could be largely separated on Fat ICD.

Fat-PCP signaling is conserved from *Drosophila* to mammalian

We establish that the human Fat homologue Fat4 lacks the ability to transduce Hippo signaling in *Drosophila*, but can transduce *Drosophila* PCP signaling, indicates that there are conserved mechanisms of Fat-PCP signaling involving the Fat ICD. And we figure out a conserved 'F' motif to be accountable for at least a portion of Fat-PCP activity.

Identify candidate Dco phosphorylation sites

Fat-Hippo signaling requires *discs overgrown* (Dco), and we characterize candidate Dco phosphorylation sites in the Fat intracellular domain whose mutation impairs Fat-Hippo signaling. Motif 'D' and phosphorylation sites mutant 'mV' impairs both Fat-Hippo signaling and Fat protein phosphorylation. Although this motif overlaps with Dco binding sites, it doesn't compromise Dco binding to Fat.

Dachs membrane polarization correlated with Fat activities

Through characterization of Dachs localization under distinct Fat signaling, we established that the control mechanism of whether Dachs is polarized can be uncoupled from the mechanism controlling the direction Dachs is polarized. And the correlation between increased membrane Dachs level with impaired Hippo activity (in FatΔD, Fat:Fat4), suggests the amount of Dachs on the membrane influences Hippo signaling. Then through directly targeting Dachs to membrane by fusing it to Zyx, phenotypes similar to *fat* null mutant were obtained, suggesting localization of Dachs transduces both Fat-Hippo and Fat-PCP signaling.

Figures

Figure 1. The Hippo signaling pathway.

Schematic depictions of the regulatory interactions among genes linked to Hippo signaling. Pointed arrows indicate a positive regulatory connection; blocks indicate an inhibitory regulatory connection. Genes depicted in red can function as tumor suppressors, genes depicted in green can function as oncogenes , genes depicted in black have not been shown to function as tumor suppressors or oncogenes. At the bottom, genes depicted in gray encode DNA binding proteins that can partner with Yki/Yap to influence transcription of downstream target genes. (adapted from Irvine K.D.)

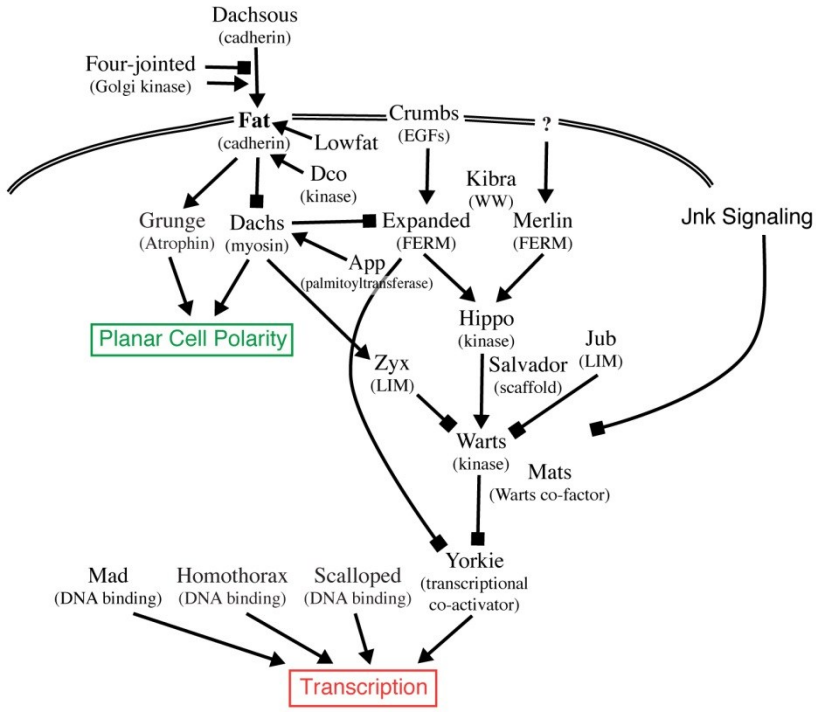

Figure 1

CHAPTER II

Zyxin Links Fat Signaling to the Hippo Pathway

Cordelia Rauskolb, Guohui Pan, B.V.V.G. Reddy, Hyangyee Oh and Kenneth D. Irvine

Results descripted in the chapter were published in

Cordelia Rauskolb, Guohui Pan, B.V.V.G. Reddy, Hyangyee Oh and Kenneth D. Irvine, *Zyxin links fat signaling to the hippo pathway.* PLoS Biol, 2011. **9**(6): p. e1000624.

Authors Contribution:

Cordelia Rauskolb, Guohui Pan, B.V.V.G. Reddy, Hyangyee Oh and Kenneth D. Irvine conceived and designed the experiments. Cordelia Rauskolb, B.V.V.G. Reddy, and Hyangyee Oh completed the RNAi screen. Cordelia Rauskolb conducted genetic characterization of Zyx. Guohui Pan investigated the molecular interaction amongst Zyx, Dachs, and Wts.

Summary

To improve understanding of the Fat-Hippo signaling pathway, we conducted an RNAi lines screen to identify additional pathway components. We identified Zyx (*Zyx102*) as an essential component of Fat-Hippo signaling. Depletion of Zyx in *Drosophila* wing discs using RNAi decreases the wing size, and down-regulates Hippo signaling targets ex-laZ, th-laZ, and DIAP1. Epistasis analysis put Zyx between Dachs and Wts in the Fat-branch: Zyx-Wts double RNAi displays a phenotype identical to Wts-RNAi. Zyx-RNAi could suppress the overgrowth phenotype caused by Fat-RNAi, Dco^3, and overexpression of Dachs. And biochemically, Zyx-RNAi suppresses the reduction of Wts level by fat RNAi. Zyx partially co-localizes with Dachs. And unlike Dachs, its localization was not altered by manipulating other Fat-branch component: neither does manipulating Zyx affect Dachs localization. Thus Zyx exerts its function by regulating Wts protein level in vivo. Zyx protein binds to Dachs, and Dachs stimulates binding of Zyx to Wts, suggesting a molecular mechanism for how Fat signaling regulates Wts through Wts. Our results identified a new component of Fat signaling, investigated its genetic relationship with other Fat pathway components, and proposed possible molecular mechanism for signal transduction from Fat to Wts.

Introduction

From LIM domain and other motif comparisons, Zyx may represent the vertebrate Zyxin, paralogous class Lipoma preferred partner (LPP), and Thyroid-receptor interacting protein 6 (TRIP6); while Jub may represent Ajuba, LIM Domains Containing 1 (LIMD1) and Wilms tumor protein 1 interacting protein (WTIP) [48, 49]. These 3-LIM domain family members feature three carboxy-terminal LIM domains, proline-rich motifs, and potential nuclear export signals in the amino-terminal two-thirds of the protein [49]. Zyxin/Ajuba family proteins have been reported to be involved in maintaining cell structure, cell fate, and differentiation [50]. Gene-targeted mutations in murine *Zyxin* or *Lpp* have no significant effect on mouse developments, presumably due to redundancy among family members [61, 62]. Translocations involving *Lpp* identified it as an oncogene involved in lipomas and other cancers [63]. Zyxin is a regulator of actin filament assembly, and proper localization of Zyxin to focal adhesions is necessary for the accumulation of ENA/VASP proteins to these sites [50, 51]. Zyxin and Ajuba could shuttle between sites of focal adhesions/cell-cell contacts and the nucleus [52-54]. Although the exact reason for cycling is not known, it has been speculated to involve transducing signals from the sites of attachment to the nucleus [55]. During mitosis, Zyxin is targeted to mitotic apparatus, and interacts with mitotic regulators *Lats1* [56, 57]. LIMD1 is also phosphorylated during mitosis [55]. Zyxin could also transit to nucleus in response to mechanical stimuli, and is required for mechanosensitive gene expression [58]. Ajuba functions as nuclear receptor co-repressor and negatively regulates retinoic acid signaling [59].

The *Drosophila* Jub is reported to serve as a negative regulator of Hippo pathway activity [48]. The epistasis analysis suggests that Jub acts upstream of Wts and Yki but downstream of Hpo. And Jub/Ajuba binds to Wts/LATS1/LATS2 and Sav/WW45, but not Hpo/Mst1. More intriguingly, human LIMD1 (most closely related to Jub) suppress the phospho-Yap level induced by MST1, WW45, and LATS1/2. In mammalian cells, Zyxin binds to LATS1 during mitosis or after Cdc2 promoted phosphorylation [56].

Materials and Methods

Drosophila genetics

RNAi screening was conducted using lines from the NIG (http://www.shigen.nig.ac.jp/fly/nigfly/index.jsp), which were crossed to *vg-Gal4 UAS-dcr2* or *pnr-Gal4 UAS-dcr2*. Those with growth phenotypes were then re-screened for effects on Diap1 and Wg expression in imaginal discs by crossing to *ci-Gal4 UAS-dcr2* or *en-Gal4 UAS-dcr2*. All crosses were carried out at 28.5C to obtain stronger phenotypes.

Additional RNAi lines employed include *ds* [vdrc 36219], *fat* [vdrc 9396], *d* [vdrc 12555], *ex* [vdrc 22994], *Zyx* [NIG-32018R3], *Zyx* [vdrc 21610], *wts* [vdrc 9928], *wts* [NIG-12072R1], *mats* [vdrc 108080], *hpo* [vdrc 104169], *Jub* [vdrc 101993], *Jub* [vdrc 38442]. The effectiveness of *fat* and *ex* RNAi is confirmed (Data not shown). Both *Zyx* RNAi lines gave similar effects on growth and gene expression in combination with multiple Gal4 lines, and also behaved similarly in epistasis tests. UAS lines employed include *UAS-dco*^{3} [48] [46], *UAS-d:V5[9F]* and *UAS-d:V5*[50-5] [38], *UAS-d:citrine[28]*, and *UAS-Zyx:V5[4]*. Gal4 lines employed include *Dll-Gal4, ex-lacZ en-Gal4 UAS-GFP/CyO;UAS-dcr2/TM6b*, *en-Gal4/CyO*; *th-lacZ UAS-dcr2/TM6b*, *ci-Gal4 UAS-dcr2[3]/TM6b*, *w UAS-dcr2[X]; nub-Gal4[ac-62]*, *w; AyGal4 UAS-GFP/C yO;UAS-dcr2/TM6b*, *y w hs-FLP[122]; AyGal4 UASGFP/CyO*, *tub-Gal80ts /CyO,Act-GFP ; tub-Gal4 UAS-dcr2/ TM6b*, *w; tub-Gal4/ CyO-GFP*. MARCM clones were made by crossing *y w hs-FLP[122] tub-Gal4 UAS-GFP/FM7 ; tub-Gal80 FRT40A/CyO* to *fat8 FRT40A/CyO*, *ex FRT40A/CyO*, *dGC13 FRT40A/CyO* or *y+ FRT40A* (as a control); *UAS-zyxin:V5*. Flp-out clones were made by crossing *y w hs-FLP[122]; AyGal4 UAS-*

GFP to *UAS-zyxin:V5* or crossing *AyGal4; UAS-d:citrine* to *yw hs-FLP[122]; UASzyxin:V5*.

Adult wing phenotypes were scored by crossing *UAS-dcr2; nub-Gal4* females to males of RNAi lines, or Oregon-R males as a control. Wings of male progeny were photographed, all at the same magnification.

Histology

For analysis of gene expression in imaginal discs, *ex-LacZ en-Gal4 UAS-GFP; UAS-dcr2* females were crossed to RNAi line males, and larvae were kept at 28.5C until dissection. For analysis of Zyx:V5 localization, expression was driven by *en-Gal4, AyGal4*, or *tub-Gal4*. Discs were fixed in 4% paraformaldehyde and stained using as primary antibodies: goat anti-ß galactosidase (1:1,000, Biogenesis), mouse anti-Diap1 (1:200, B. Hay), rat anti-E-cad (1:200, DSHB), guinea pig anti-Ex (1:2000, R. Fehon), rat anti-Fat (1:400)28, mouse anti-V5 (1:400, Invitrogen), mouse anti-Wg (1:400, DSHB), and rabbit anti-Yki (1:400)21. F-actin was stained using Alexa Fluor 546 phalloidin (1:100, Invitrogen), and DNA was stained using Hoechst (Invitrogen).

For analysis of Wts protein levels, *tub–Gal4 UASdcr2/ TM6b* females were crossed to *RNAi-fat*, *RNAi-Zyx* or *RNAi-fat*; *RNAi-Zyx* males, and wing discs were dissected from third instar larval progeny.

Plasmid constructs

UAS-Zyxin: Full length zyxin cDNA (2021bp, including 5'UTR, CDS (nt181-nt1938, which is 1-585aa) and 3'UTR) were amplified by PCR from cDNA clone *zyx102.44* 10 (plasmid pEXlox44a from Beckerle [49], 2021bp; also deposited as GenBank AF219948), (using the forward primer: 5'-

AATTCGTTAACAGATCTGCGGCCGCATAAATTCGATAAGCGATAG-3' and the reverse primer: 5'-CCTCTAGAGGTACCCTCGAGTTTTTTTATTATTATCAATTTATTTTCCGA-3'), and cloned into NotI/XhoI digested pUAST-attB.

UAS-Zyxin:V5: A V5-epitope-tag, with poly-glycine linker, was PCR amplified (using oligonucleotides: 5'-CCGCATGACGTCAGAACATGGAGGAGGAGGAGGTAAGCCTATCCCTAA- 3' and 5' –TAAAATGAGCACTCAATTTAACCGGTACGCGTAGAATCGAGA-3'), and added directly carboxy-terminal to the last amino acid of Zyxin (585aa) by QuikChange Site-Directed Mutagenesis Kit (Stratagene) to make UAS-Zyxin:V5.

UAS-Zyx-LD:V5: using UAS-Zyxin:V5 as template, nt1336-nt2021 (386aa-585aa and 3'UTR) was amplified by PCR, with an ATG added (using the forward primer: 5'-TAACAGATCTGCGGCCGCATGGGTAGGTGTGTCAAATGCA-3' and the reverse primer: 5'-CCTCTAGAGGTACCCTCGAGTTTTTTTATTATTATCAATTTATTTTCCGA-3'), then cloned into NotI/XhoI digested pUAST-attB to make UAS-Zyx-LD:V5.

These constructs were injected into PhiC31 attP2 (68A4 on 3rd chromosome) site. The insertion events were verified by PCR. And multiple independent transformants are tested to make sure that they show the same phenotype.

UAS-Flag:Zyxin: to add N-terminal 3 FLAG tags, Full length zyxin (nt184-nt2021, which is 2-585aa and 3'UTR), zyxin LIM domain(nt1336-nt2021, which is 386-585aa and 3'UTR), and zyxin N-terminal(nt184-nt1335, which is 2-385aa) were amplified by PCR from cDNA clone *zyx102.44* (pEXlox44a [10]), (using forward primer: 5'-

CGCGGTACCGAGTCTGTGGCCCAGCAACTTA-3', 5'-CGCGGTACCGGTAGGTGTGTCAAATGCA-3', and reverse primer: 5'-TGCACTAGTTTTTTTATTATTATCAATTTATTTTCCGA-3', 5'-TGCACTAGTTTAGTAGTTTTCCAATTCTTGAACC-3'), then cloned into KpnI/XbaI digested pUAST-FlagCG13139 (Mao, lft paper), replacing the *lft* insertion.

UAS-Flag:Ajuba is made the same way as UAS-Flag:Zyxin: to add N-terminal 3 FLAG tags, Full length Ajuba (1-728aa), Ajuba LIM domain(467-728aa), and Ajuba N-terminal(1-466aa) were amplified by PCR from pUAST-mCherry-dJuba, (using forward primer: 5'-CGCGGTACCATGACCACCCAGCGGACGCAGAC-3', 5'-CGCGGTACCGGTCTCACCAAGAATCTGCTA-3', and reverse primer: 5'-TGCACTAGTTTATCTCCTGGGTTTCAAGGCA-3', 5'-TGCACTAGTTTATCCCATATACTGGTACGAA-3'), then cloned into KpnI/XbaI digested pUAST-FlagCG13139 (Mao, lft paper), replacing the *lft* insertion.

Flag:wts: similarly, Full length wts (pUAST-Wts:FLAG), N-terminal 708aa (pUAST-WtsΔC398:FLAG), N-terminal 192aa (pUAST-WtsΔC914:FLAG), C-terminal 914aa (pUAST-WtsΔN192:FLAG), C-terminal 398aa (pUAST-WtsΔN708:FLAG) were amplified by PCR from pUAST-wts-Myc (Tian Xu), and cloned into KpnI/XbaI digested pUAST-FlagCG13139 (Mao, lft paper), replacing the *lft* insertion.

pUAST-Dachs:V5 has been described previously.

pUAST-Dachs-M:V5: nucleotides 867-3216 of GenBank CG10595-PA was PCR amplified, with ATG added, and inserted into EcoRI/XbaI digested pUAST-Dachs:V5 to replace the full length Dachs cDNA with this myosin domain only cDNA.

All plasmid constructs were verified by DNA sequencing.

Co-immunoprecipitation and western blotting

Co-immunoprecipitation assays were performed as described previously [46]. S2 cells were cultured with Schneider's *Drosophila* medium (Invitrogen) and 10% FBS (Sigma). Transfections were performed with Cellfectin II (Invitrogen) according to the manufacturer's protocol. Generally, 500-750ng of each plasmid was used for transfecting 0.3-0.5x10^6 Cells in a 10cm^2 well. For Zyx-LD, 1500-2000ng was used to compensate its lower expression level. Cells were harvested 36-60h after transfection, washed once with cold PBS and lysed with freshly prepared RIPA buffer (50mM Tris-HCl, pH8.0; 150mM NaCl; 1% NP-40; 0.5% Na deoxycholate; 0.1% SDS; 0.4mM EDTA; supplemented with protease inhibitor cocktail (Roche) and phosphatase inhibitor cocktail SetII (CalBiochem). Cell lysate is pre-absorbed by protein G beads (Sigma). Anti-V5 beads (Sigma) or Anti-FLAG M2 beads (Sigma) were mixed with cell lysate and incubated overnight at 4 °C, then washed six times with RIPA buffer and boiled in SDS-PAGE loading buffer. Primary antibodies used for blotting include Rabbit anti-V5 (1;10,000, Bethyl), mouse anti-V5 (1:10,000, Invitrogen), and mouse anti-FLAG M2-HRP (1:10,000, Sigma). Fluorescent detection was performed on a LiCor Odyssey, using goat anti-mouse IRdye680 and goat anti-rabbit IRdye800 (1:10,000, LiCor).

Results

Zyx as a new component of Fat-Hippo signaling

From an RNAi lines screen to identify additional pathway components. We identified Zyx (*Zyx102*) as a novel component of Fat-Hippo signaling. There is no *Zyx* null allele available, thus most of our studies relies on RNAi lines *NIG-32018R3* and vdrc 21610. These two RNAi lines give similar results, although *NIG-32018R3* has slightly stronger phenotype. And both of them could be rescued by overexpression of Zyx from a UAS transgene, confirming that the phenotypes are specific from reduction of *Zyx*.

We employed multiple Hippo activity assays to analyze whether this pathway requires *Zyx*. Depletion of Zyx in *Drosophila* wing discs using RNAi decreases the wing size, renders shorter legs, which are regulated by Hippo signaling. Reduction of Zyx also down-regulates ex-lacZ, th-laZ, and DIAP1, which serve as reporters for Hippo signaling target gene *expanded* expression and *th* expression. Yki is the downstream effector of Hippo signaling, *Zyx* RNAi reduces Yki nuclear localization. Thus, *Zyx* is an essential component of Hippo signaling. And unlike other components, *Zyx* positive regulates Hippo signaling activity.

There are multiple upstream branches in Hippo pathway, epistasis analysis puts Zyx between Dachs and Wts in the Fat-branch: *Zyx/wts* double RNAi displays a phenotype identical to *wts* RNAi. *Zyx* RNAi could suppress the overgrowth phenotype caused by Fat-RNAi, Dco^3, and overexpression of Dachs. And biochemically, Zyx-RNAi increases the level of Wts, and suppresses the reduction of Wts level by *fat* RNAi. Fat signaling has PCP activities. Nevertheless, *fat Zyx* double RNAi can't suppress the PCP phenotype of

fat RNAi, and *Zyx* RNAi itself doesn't impair PCP. These observations indicate *Zyx* is specifically required for Fat-Hippo signaling, not for Fat-PCP signaling.

To investigate the mechanism of *Zyx* regulating Hippo signaling, we examine the localization of *Zyx*. Zyx partially co-localizes with Dachs on sub-apical membrane, but not polarized. Unlike Dachs, Zyx localization was not altered by manipulating other Fat-branch component; neither does manipulating Zyx affect Dachs localization.

Dachs promotes Zyx-Wts binding

The similar genetic requirements for *Zyx* and *dachs* in Fat-Hippo signaling, together with their partial co-localization in imaginal discs, raised the possibility that Zyx and Dachs might directly interact. This was investigated by expressing tagged isoforms in cultured *Drosophila* S2 cells, and assaying for physical interactions through co-immunoprecipitation. Indeed, Zyx and Dachs could be specifically co-precipitated from S2 cells (Figure 1B), which implies that the co-localization observed in vivo reflects direct physical interaction between them.

As Dachs can also bind to Warts in co-immunoprecipitation assays [21], and both *Zyx* and *dachs* are required for the *fat*-dependent regulation of Wts levels, we also investigated binding between Zyx and Wts. When tagged full-length proteins were co-expressed in S2 cells, Zyx-Wts binding was close to background levels (Figure 1C). However, it was reported that the C-terminus of human Zyxin, including the LIM domains, could bind to human LATS1, even though full length Zyxin did not bind [56]. When we expressed a C-terminal polypeptide comprising the LIM domains of Zyx in S2 cells, only very low levels of protein could be detected, suggesting that this polypeptide is unstable (Figure 1B-D). Nonetheless, this C-terminal polypeptide bound efficiently to

Wts (Figure 1C). Thus, the LIM domains of Zyx can associate with Wts, but this association is normally masked within full-length Zyx.

The discovery of this latent ability of Zyx binding Wts, together with our discovery of Zyx-Dachs binding, and previous identification of Dachs-Wts binding, indicates that Dachs, Zyx, and Wts each have the ability to bind to one another. To gain further insight into complex formation among these proteins, we mapped their interaction domains (Figure 1A). Wts bound to the LIM domains of Zyx. Dachs by contrast, bound most strongly to the C-terminal LIM domains, but also bound detectably to the N-terminal half of Zyx (Figure 1B). Dachs contains a large central myosin domain, surrounded by unique N- and C-terminal regions. Dachs could bind to both Zyx and Wts through its myosin domain (Figure 1D). Besides the myosin domain, Zyx could also bind to N-terminal regions of Dachs. The Zyx-LD bound to Wts through a region just N-terminal to the Wts kinase domain (Figure 1E), consistent with studies of Zyxin-LATS1 binding [56]. Dachs bound both to this region, and also to the Wts kinase domain (Figure 1F). Thus, Zyx, Dachs and Wts interact with each other through partially overlapping domains.

To assay for potential sequential, cooperative, or competitive interactions among Zyx, Dachs, and Wts, we examined binding interactions when all three proteins were co-expressed together in S2 cells. A key feature of Zyx's interactions with Wts is that full length Zyx does not bind efficiently to Wts, but the LIM domains do. However, we found that Dachs enhanced the co-precipitation of full length Zyx with Wts (Figure 1G). Two basic models for this stimulation of Zyx-Wts association by Dachs can be envisioned: a) Dachs might bridge Wts and Zyx in a trimeric Wts-Dachs-Zyx complex, b) Dachs might trigger a conformational change in Zyx that reveals the latent Wts-binding activity of the

Zyx LIM domains (Figure 3). By employing V5 epitope tags on both Zyx and Dachs, and assaying their co-precipitation with FLAG-tagged Wts, we could directly compare their association with Wts. A simple trimeric complex model (e.g. one subunit each of Zyx, Wts, and Dachs) would predict that Zyx and Dachs should be present within the complex at equal levels. However, we found instead that Zyx was much more abundant in Wts complexes than was Dachs (Figure 1G). Moreover, Dachs did not stimulate the binding of a Zyx LIM-domains-only polypeptide to Wts (Figure 2), implying that after exposed, Zyx LIM domain no longer requires Dachs. These observations suggest that rather than remaining stably associated with Zyx and Wts in a trimeric complex, Dachs is able to act catalytically, stimulating a conformational change in Zyx that exposes the LIM domains and enables them to bind Wts.

DISCUSSION

We identified Zyx as a novel component of *Drosophila* Fat-Hippo pathway, and genetic positioned it between *dachs* and *wts*. Dachs, Zyx and Wts could bind one another, and intriguingly, Dachs could stimulate the binding between full length Zyx and Wts. Similar interaction is also evident in vertebrate, as the LIM domain, but not full length Zyxin could bind to LATS1, and Cdc2-mediated phosphorylation could stimulate full length Zyxin binding. We propose Dachs might catalyze a conformational change of Zyx to expose the LIM domain, or induce post-translational modification of Zyx. Further investigation is needed to reveal the detailed mechanism.

The *Drosophila* Jub is reported to serve as a negative regulator of Hippo pathway activity [48]. Epistasis tests indicate *Zyx* and *Jub* regulate Wts in distinct ways. *Jub* is required for both Fat-Hippo and Ex-Hippo signaling, and act genetically between *hippo* and *wts*. This is also reflected in distinct biochemical interactions. By contrast to the critical role of Dachs in stimulating binding between full length Zyx and Wts, full length Jub binds efficiently to Wts, and full length vertebrate homologues of Jub bind to LATS proteins [48, 64]. Moreover, Jub binds much weaker to Dachs than Zyx does (Figure 2B). Thus, although *Zyx* and *Jub* share the ability to associate with Wts through their LIM domains, both genetic and biochemical studies indicate that the regulation and consequences of these LIM-domain-Wts interactions are distinct.

One of the most intriguing aspects of Zyxin family proteins is their role in mediating effects of mechanical force on cell behavior [65]. Zyxin family proteins can localize to focal adhesions of cultured fibroblasts, and this localization is modulated by mechanical tension [65, 66]. The observation that increasing tension on stress fibers stimulates Zyxin

accumulation at focal adhesions is intriguing in light of the observation that Zyx tends to accumulate at higher levels at intercellular vertices [60], these could be points of increased tension. The basis for the tension-dependent recruitment of Zyxin to focal adhesions is unknown [65]. As the association of unconventional myosins with F-actin can also be influenced by external force [67], our discovery of binding between a myosin protein (Dachs) and Zyx raises the possibility that other myosins might also interact with Zyxin family proteins, which could potentially provide a mechanism for their tension-based recruitment to focal adhesions or adherens junctions.

Finally, we note that theoretical models of growth control in developing tissues have proposed that growth should be controlled by mechanical tension [68, 69], but a mechanism for how this might be achieved has been lacking. Our discovery that Zyx, a member of a family of proteins implicated in responding to and transducing the effects of mechanical tension, is also a regulator of the Hippo signaling pathway, a crucial regulator of growth from *Drosophila* to humans, now suggests a potential mechanism by which mechanical tension might be linked to growth in developing tissues.

Figure

Figure 1. Binding amongst Zyx, Dachs, and Wts.

(A) Schematic of Wts, Dachs, and Zyx proteins, and the constructs used to map interaction domains. LD indicates LIM Domain. Binding interactions are summarized to the right; + indicates strong binding, and − indicates weak or no binding. (B–G) show Western blots on co-immunoprecipitation experiments, with upper two blots indicating the relative amount of protein in the lysates used for the experiments and the lower panel indicating the material co-precipitated by the indicated antibody. GFP serves as a negative control. In (B–D) arrow identifies the Zyx-LD:FLAG polypeptide, and other bands in this lane are non-specific background detected by the antibodies. (B) Co-precipitation of V5-tagged Dachs with the FLAG-tagged proteins indicated at top. (C) Co-precipitation of FLAG-tagged Wts with the V5-tagged proteins indicated at top. (D) Co-precipitation of V5-tagged Dachs myosin domain with the FLAG-tagged proteins indicated at top. (E) Co-precipitation of V5-tagged Zyx-LD polypeptide with the FLAG-tagged proteins indicated at top. (F) Co-precipitation of V5-tagged Dachs with the FLAG-tagged proteins indicated at top. (G) Co-precipitation of FLAG-tagged Zyx with the V5-tagged proteins indicated at top. (H) Co-precipitation of V5-tagged Dachs and Zyx with the FLAG-tagged proteins indicated at top, in the presence of increasing amounts of Dachs:V5, as indicated. 1x indicates that equal amounts of pUAS-Zyx:V5 and pUAS-dachs:V5 plasmids were used, and 3x and 6x indicate corresponding increases in amounts of pUAS-dachs:V5 plasmid transfected. Note that in the absence of Dachs, no binding between full-length Zyx and Wts was detected when proteins were precipitated using anti-V5 beads and GFP:V5 was used as a negative control (panel C), but weak

binding was detected when proteins were precipitated using anti-FLAG beads and GFP:FLAG was used as a negative control (H).

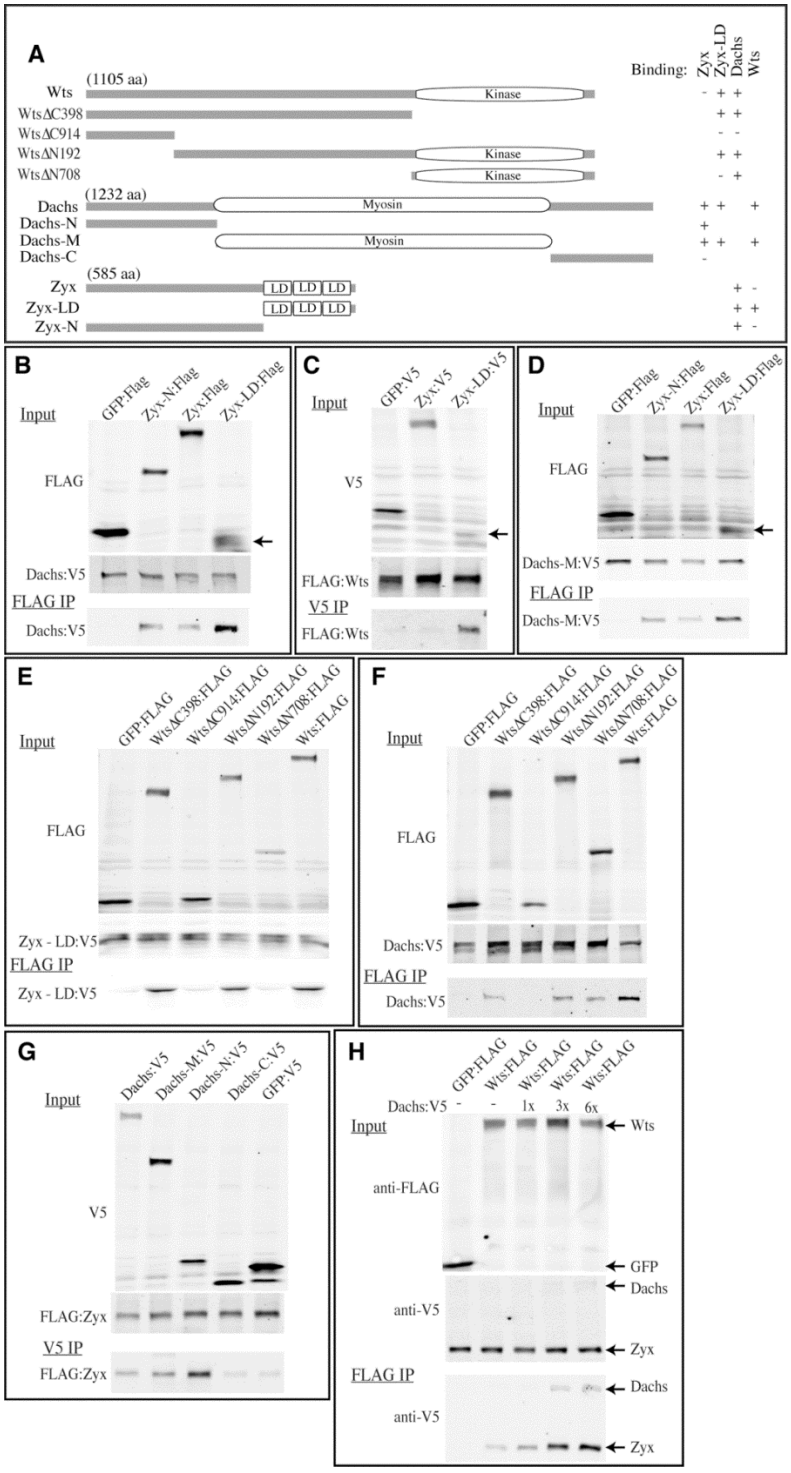

Figure 1

Figure 2. Additional studies of binding amongst Zyx, Jub, Dachs, and Wts. Western blots on co-immunoprecipitation experiments, with upper two blots indicating the relative amount of protein in the lysates used for the experiments, and the lower panel indicating the material co-precipitated by the indicated antibody. GFP serves as a negative control. (A) Co-precipitation of V5-tagged Dachs and Zyx-LD with the FLAG-tagged Wts or GFP control, as indicated at top. Addition of Dachs:V5 (3x refers to amounts used in Figure 1H) does not increase precipitation of Zyx-LD with Wts. Arrows identify the indicated proteins. (B) Co-precipitation of V5-tagged Dachs with the FLAG-tagged proteins indicated at top. The results show that Dachs binds to Zyx much more strongly than it does to Jub.

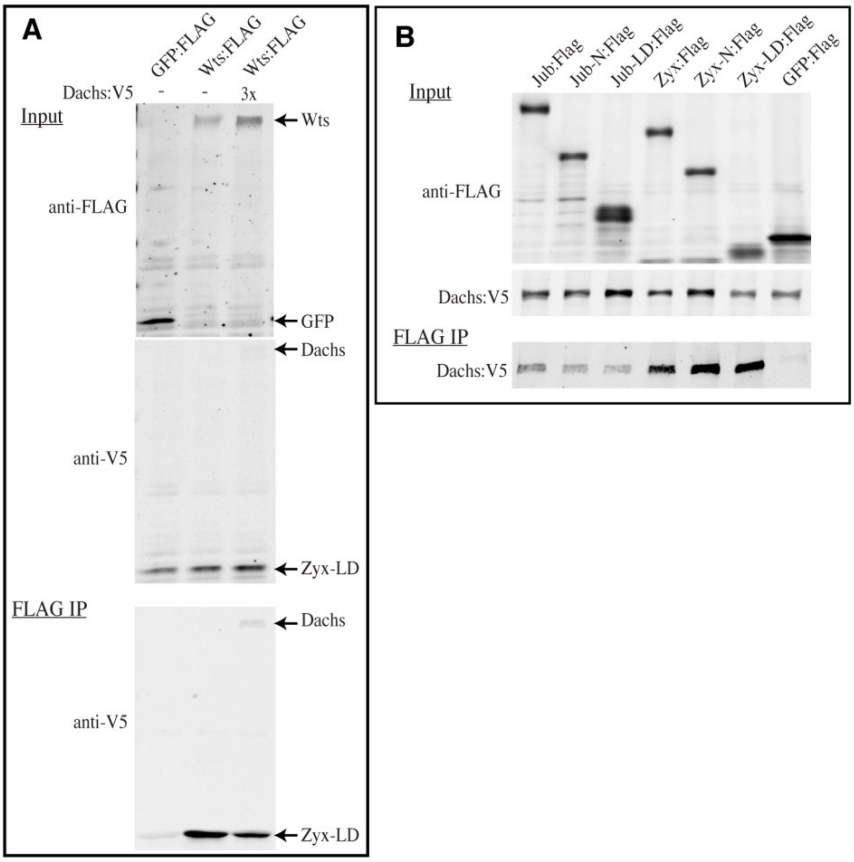

Figure 2

Figure 3. Models for Zyx function in Fat-Hippo signaling

A) Dachs might bridge Zyx and Wts in a trimeric complex; this model would predict the three proteins to be present in stoichiometric amounts, which was not observed. B) Dachs might induce a conformational change in Zyx, exposing the LIM domains and enabling it to bind Wts. C) Illustrates the distinct roles of the LIM-domain proteins Zyx and Jub in Hippo signaling. Zyx influences the levels of Wts protein, presumably by promoting Wts degradation, whereas Jub inhibits Wts activation.

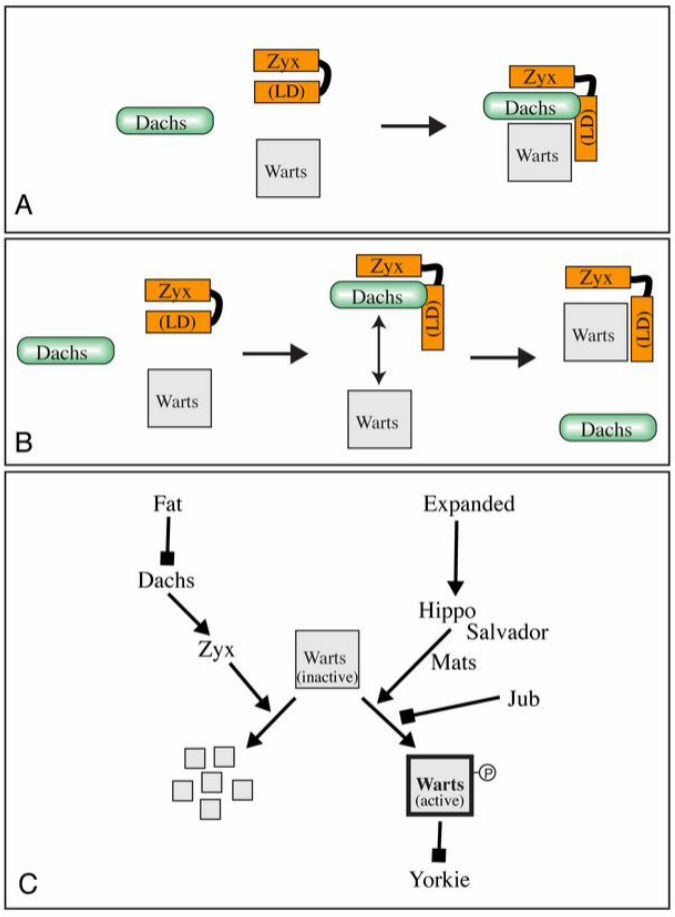

Figure 3

CHAPTER III

Signal transduction by the Fat cytoplasmic domain

Guohui Pan, Yongqiang Feng, Abhijit A. Ambegaonkar, Gongping Sun, Matthew Huff, Cordelia Rauskolb, and Kenneth D. Irvine

This chapter was published in

Guohui Pan, Yongqiang Feng, Abhijit A. Ambegaonkar, Gongping Sun G, Matthew Huff, Cordelia Rauskolb, Kenneth D. Irvine. *Signal transduction by the Fat cytoplasmic domain.* Development. 2013 Feb;140(4):831-42.

Authors Contribution:

Guohui Pan, Yongqiang Feng, Abhijit A. Ambegaonkar, Gongping Sun, Cordelia Rauskolb, and Kenneth D. Irvine conceived and designed the experiments. Guohui Pan created the Fat intracellular domain motif mutations, conducted most phenotype characterizations and biochemical assays. Yongqiang Feng created wild-type Fat, Fat:Fat4, FatΔICD, FatP32 genomic constructs, and identified potential Dco phosphorylation sites. Gongping Sun constructed Fat-mI, Fat-mIV, and Fat-mV. Matthew Huff analyzed the intercellular ridges. Abhijit A. Ambegaonkar and Cordelia Rauskolb investigated the influence of directed Dachs membrane localization. Binnaz Kucuk created Myr:Dachs. Tahia Haque assisted in preliminary characterization of *fat* deletion constructs

Summary

Organ morphogenesis requires coordination of growth and patterning control, which orients cell behavior. Among the vast amount of genes involved in either growth or patterning control, Fat gene stands out as its ability to transduce both growth cues (through Hippo signaling) and planar cell polarity (PCP). But the molecular mechanism underlying is unknown. To investigate how Fat regulates distinctive pathways, a structure-function approach is recruited to figure out the motifs in Fat that are required for Hippo signaling/growth control, Dachs localization, and regulation of PCP, thus to shed light on the signal transduction mechanism.

Instead of over-expressing truncated or mutated cDNA under exogenous promoters, I take advantage of a *fat* genomic Bac Clone, which is expressed under endogenous condition and reveal activities that could be missed when proteins are over-expressed. By this technique, we find out the PCP activity is evolutionarily conserved from *Drosophila* to mammals. The human FAT4 ICD could transduce PCP activity but not Hippo activity. And in the *Drosophila fat* gene, Hippo and PCP activity can be largely separated at the level of the Fat receptor. A specific motif was identified to mainly impair Fat-Hippo activity and reduce Fat phosphorylation. Manipulating the potential phosphorylation sites in this motif gives similar phenotypes, implicating phosphorylation as an essential factor in Fat-Hippo signaling transduction. This motif overlaps with the previously identified Dco binding site, but retains normal binding affinity.

Another conserved four amino acid motif is found to be crucial for Fat-PCP, while the Fat-Hippo activity is almost normal. And this motif contributes differently to multiple PCP assays, suggesting there are different kinds of PCP in *Drosophila*.

It has been proposed that the influence of Dachs on Fat-Hippo signaling is related to the amount of Dachs localized to the membranes, whereas its influence on Fat-PCP is related to the direction in which Dachs membrane localization is polarized. We show that losing different Fat activity leads to distinctive Dachs localization pattern, and directly manipulating Dachs localization could phenocopy loss of Fat activity. Thus we provide direct evidence that Dachs localization influences both Hippo and PCP phenotypes. Our results identify a conservation of Fat PCP signaling mechanisms, establish distinct functions for different regions of the Fat ICD, support the correlation of Fat ICD phosphorylation with Fat-Hippo signaling, and confirm the importance of Dachs membrane localization to downstream signaling pathways.

Introduction

How the growth and patterning of tissue development are controlled and coordinated has been one of the fundamental questions in developmental biology. Fat is a large atypical cadherin protein serving as a transmembrane receptor for signal transduction pathways that regulate growth (Hippo signaling) and PCP [5, 22, 29]. Fat is regulated by two proteins expressed in gradients: Ds and Fj. Ds encodes an atypical cadherin that can function as a ligand for Fat [5, 22, 29]. Fj is a Golgi-localized kinase that phosphorylates cadherin domains of Fat and Ds to modulate binding between them [34, 35, 70]. Rather than responding solely to the level of Ds and Fj, Fat is also regulated by the slope and vector of their expression gradients, with the slope influencing Hippo signaling and the vector influencing PCP [36, 37, 71].

Fat is one of several upstream pathways that impinges on Hippo signaling [8, 23, 72]. Most of these upstream inputs converge on the kinase Wts, which negatively regulates the transcriptional co-activator Yki. Hippo pathway activity promotes Wts activity, which promotes cytoplasmic localization of Yki. When *fat*, *wts*, or other upstream tumor suppressors are down regulated, then Yki accumulates in the nucleus, increasing transcription of genes that promote growth. Three genes have been identified as playing key roles in Fat-Hippo signal transduction: *dco*, *dachs*, and *Zyx*.. An antimorphic allele, dco^{3}, specifically impairs Fat-Hippo signaling [21, 46]. A portion of Fat is phosphorylated on its intracellular domain (ICD); this phosphorylation depends upon both Ds and Dco, suggesting that Fat ICD phosphorylation is a key step in Fat-Hippo signal transduction [46, 47]. Dachs is a myosin that down regulates Wts, and is required for the influence of *fat* or *dco* mutations on Hippo signaling [21, 73]. Dachs localization is normally polarized in response to the Ds and Fj

gradients [36, 38, 74-76]. When Fat is over-expressed, Dachs membrane localization is reduced, whereas when Fat is mutant, Dachs localizes to the membrane around the entire circumference of the cell [38]. The correlation between Dachs localization and Fat activity suggests that regulation of Dachs localization is a key step in Fat signal transduction. Zyx affects Fat-Hippo signaling similarly to Dachs [60]. Zyx and Dachs can bind each other, and binding of Dachs to Zyx stimulates Zyx-Warts binding [60].

Dachs participates in both Fat-Hippo and Fat-PCP pathways, but it has been proposed that the influence of Dachs on Fat-Hippo signaling is related to the amount of Dachs localized to the membrane, whereas its influence on PCP is related to the direction in which Dachs membrane localization is polarized [29, 36]. One manifestation of Fat-PCP in the wing is the orientation of cell divisions, which contributes to wing elongation. In *fat*, *ds*, or *dachs* mutants, cell division orientation is randomized, resulting in rounder wings [27, 77]. It has been proposed that Dachs myosin motor activity may contribute to the orientation of wing cell division by contracting cell apices, thereby altering cell geometry [77]. Modulation of tension along intercellular junctions also appears to contribute to influences of Dachs on PCP in the notum [75]. A transcriptional co-repressor, Atrophin, has also been linked to some Fat-PCP phenotypes [78, 79].

The central core of the Hippo pathway is conserved between *Drosophila* and mammals, but there is variation amongst upstream regulators [8, 9]. Vertebrates have homologues of Fat (Fat4) and Ds (Dchs1), and depletion of Fat4 could affect Yap activity in a subset of CNS neurons in chicks [80]. However, gene-targeted mutations in *Dchs1* or *Fat4* do not result in evident Hippo pathway phenotypes in mice, although they are consistent with influences of *Dchs1* and *Fat4* on PCP [31, 81]. Mammals do not, however, have an obvious Dachs

homologue, and it remains unclear whether Fat signaling pathways in flies and mammals are related.

Here, we employ a structure-function approach to investigate signal transduction downstream of Fat. We show that Hippo and PCP pathways can be separated at the level of the Fat receptor. We identify point mutations in the Fat ICD that specifically impair Fat-Hippo signaling and reduce Fat phosphorylation, and identify a conserved four amino acid motif that is crucial for effects of Fat on PCP. We also explore the relationship between Fat signaling and Dachs localization and provide direct evidence that Dachs localization influences both Hippo and PCP phenotypes.

Materials and Methods

Drosophila genetics

Rescuing activity of fat transgenes was characterized by crossing *fat^{GrV}/CyO,GFP; P[acman]-ft*/TM6b or ft^{8}/CyO,GFP; P[acman]-ft*/TM6b* to *ft^{Grv}/CyO.GFP, ft^{8}/CyOActGFP*, or ft^{GrV}/CyO,GFP; P[acman]-ft*/TM6b, where *P[acman]-ft** indicates wild-type or mutant forms of fat rescue constructs. To overexpress Wts, *ft^{8} UAS-myc:Wts /CyOGFP* and *tub-$Gal4^{[LL7]}$* chromosomes were used. Clones expressing Dachs:Cit were made by crossing *hs-FLP; ft^{GrV}/CyO,GFP; P[acman]-ft* /TM6b* to *ft^{8}/CyO,GFP;act>CD2,y+>dachs:cit/TM6b*.

To quantify wing area, male wings were traced using ImageJ, and areas were normalized to the average in controls. To quantify cross-vein distance, the length of vein L4 between cross-veins was measured using ImageJ, and divided by the length of vein L3, to get a relative length, and these were normalized to the wild-type ratio. For mutant wings with incomplete cross-veins, points of crossing were estimated where possible based on the direction of the incomplete cross-vein. Hair polarity phenotypes were evaluated by the angle of deviation from the normal axis, and categorized as <30°; 30°- 90°; or >90°, if more than 10% of wing hairs showed a deviation. Only the regions anterior to L3 and proximal to the posterior cross-vein were scored; costa and abdomens were scored independently using similar criteria. the anisotropy of Fat staining along Proximal-distal (PD) interfaces is measured in ImageJ [74].

Plasmids and Constructs

Following recombineering techniques (http://recombineering.ncifcrf.gov/), the *Drosophila* fat-ICD in the genomic construct was replaced by *galactose kinase* (*galK*) via

positive selection, and then the *galk* was recombined with PCR fragments of *Fat4*-ICDs by negative selection [82] (see Appendices for primers). Recombineering was similarly used to introduce deletion or substitution mutations. Constructs were amplified by copy induction to enhance DNA yield [83] and supercoiled DNA was then purified and inserted into attP2 on 3L [84].

Histology and imaging

Imaginal discs were fixed and stained as described previously [73], using mouse anti-Wg (1:800, 4D4, Developmental Studies Hybridoma Bank (DSHB)), rat anti-DE-Cadherin (1:40, DCAD2, DSHB), mouse anti FLAG M2 (1:400, Sigma), mouse anti-V5 (1:400 preabsorbed, Invitrogen) and rat anti-Fat (1:1600). Fluorescent stains were captured on a Leica confocal microscope. For horizontal sections, maximum projection through multiple sections was employed to allow visualization of staining in different focal planes.

Co-immunoprecipitation and western blotting

Co-immunoprecipitation from S2 cells was performed as described previously [60], using anti-FLAG M2 beads (Sigma). For anti-Fat Western blots, 3rd instar stage wing discs were lysed in SDS-PAGE loading buffer supplemented with protease inhibitor cocktail (Roche) and phosphatase inhibitor cocktail SetII (CalBiochem), and stored at -80°C. Approximately 10-14 discs were loaded per lane, and the total protein amount was adjusted by normalizing to GAPDH. Primary antibodies used for blotting include Rat anti-Fat (1: 2000), Mouse anti-GAPDH (1:10,000), Rabbit anti-V5 (1:5,000, Bethyl), and mouse anti-FLAG M2-HRP (1:10,000, Sigma). Detection was performed on a LiCor Odyssey, using goat anti-mouse IRdye680 and anti-rabbit IRdye800 (1:10,000, LiCor).

Results

It's still a mystery how Fat transduces Hippo and PCP signaling, to coordinate the growth control and patterning during organ morphogenesis. We want to shed light on the Fat-signal transduction mechanism by dissecting the motifs in Fat that are required for Hippo signaling/growth control, regulation of PCP, and Dachs localization. In *Drosophila*, people have been successfully using UAS-driven expression of truncated cDNA to reveal the physiological role of protein motifs. However, over-expression of *fat* cDNA under exogenous promoter has ligand-independent effect, and could obscure or bypass requirements for sequences that are normally essential for Fat activity, rendering precise analysis of phenotypic characters difficult. To prevent this problem, we created a genomic Bac clone containing a 39kb region encompassing the whole *fat* locus (Figure 9*A*), which could provide both Hippo and PCP activities and fully rescue *fat* null mutants [46]. Despite the greater technical difficulty of manipulating genomic construct, these genomic *fat* transgenes are expressed under endogenous chromosome environment, at similar level as endogenous *fat* gene (Figure 4). The wild-type fat transgene, either with one copy or two, could provide appropriate Hippo and PCP activity and fully rescue *fat* null mutants. Thus we favored this approach over the expression of cDNA under heterologous promoters.

Conservation of Fat-PCP signaling by mammalian Fat4

Functionally important sequence motifs can often be identified by evolutionary conservation. Among the four *Fat* genes in mammalian (Fat1-Fat4) and two in *Drosophila* (Fat and Kugelei), only human FAT4 show significant similarity in ICD region to *Drosophila* Fat [30] (Figure 8). And Fat4 is involved in vertebrate PCP

signaling [32, 85]. To assess the functional significance of this similarity, we investigated whether human Fat4 could rescue *Drosophila fat* mutants. As our goal was to investigate signal transduction by the ICD, the potential difference between the extra-cellular domains (ECD) of *Drosophila* Fat and human Fat4 was excluded, by creating a hybrid transgene in which the intracellular domain of *Drosophila Fat* is replaced by the ICD from human FAT4 (Figure 9*B*). This Fat:Fat4 hybrid was constructed within a *fat* genomic rescue construct [46] by recombineering, and inserted using phiC31-mediated site-specific recombination into the same location as the previous wild-type *Drosophila* Fat (attP2 at 68A4). [21, 83]

Then this Fat:Fat4 transgene was incorporated into *fat* null mutants (ft^{8}/ft^{GrV}) and phenotypic characterization was conducted. This Fat:Fat4 hybrid transgene could not rescue the lethality of *Drosophila fat* mutants. And wing imaginal discs from *fat* mutant larvae expressing Fat:Fat4 show overgrown imaginal discs typical of a *fat* mutant, (Figure 9D, F) indicating Fat:Fat4 hybrid lacks Fat-Hippo signaling.

As assessing PCP phenotypes requires viable adult flies, we took advantage of the observation that the lethality and overgrowth phenotypes of *fat* mutations are suppressed by Wts overexpression, whereas the PCP phenotypes could still be observed (Figure 1A, B) [86]. When Wts is over-expressed, *fat* mutation with Fat:FAT4 have normal viability (Data not shown), and similar wing size as *fat* mutation expressing Wts without wild-type Fat transgene (Figure 9A, C).

We examined several PCP phenotypes to get a comprehensive evaluation of the Fat-PCP activity. Wing hairs normally point distally, but when Fat activity is impaired, wing hairs are mis-oriented and swirling patterns can be observed in the proximal wing [87]. To quantify

effects on hair polarity, we classified wing hair PCP phenotypes as “normal” when hair orientation was within 30° of its normal distal orientation; “weak” when clusters of hairs (constituting >10% of hairs in the region examined) could be identified with an orientation that appeared to deviate more than 30° but less than 90° from normal distal orientation; and “strong” when clusters of hairs could be identified with an orientation that appeared to deviate more than 90° from normal (Figure 1M). By these criteria, 100% of *fat* mutant wings rescued by a wild-type Fat transgene have a normal PCP phenotype, whereas 100% of Wts-rescued *fat* mutant wings have a strong PCP phenotype in the proximal, anterior wing (Figure 1E, F, L). Using the same criteria, all *fat* mutant abdomens rescued by a wild-type Fat transgene have normal hair polarity, whereas all Wts-rescued *fat* mutant abdomens have a strong PCP phenotype (Figure 1H, I, K). In *fat* mutants expressing Fat:Fat4 and Wts, about 60% of wings have normal wing hair orientation, and rest 40% have weak PCP phenotype, much weaker compared to Wts-rescued *fat* mutants wings without Fat transgenes (Figure 1G, L). And Fat:Fat4 could completely rescued in the abdomen (Figure 1H, J, K), having indistinguishable abdomen hair pattern from that of *fat* mutants expressing WT Fat and Wts (Figure 1I, J, K).

Another PCP parameter examined is the reduction of the distance between the anterior and posterior cross-veins, which is a classic Fat pathway mutant phenotype (Figure 1A, B), that is proposed to reflect the influence of Fat-PCP signaling on wing elongation. Wing elongation is influenced by Fat-PCP signaling both during disc growth, when it polarizes cell divisions along the proximal-distal axis, and during pupal development, when it influences local cell rearrangements [77, 88, 89]. Fat:Fat4 partially rescued the reduced cross-vein spacing

phenotypes of *fat* mutants (Figure 1C, N), having a ratio of about 0.52 compared with 0.13 of *fat* mutants.

We also analyzed the organization of intercellular ridges within the wing, whose formation reflects polarized cellular organization [26]. Like wing hairs, ridges are influenced by both Fz and Fat-PCP pathways, however ridge orientation is regulated separately from hair polarity [90]. In wild type, wing ridges run along the proximal-distal axis in the posterior wing, but along the anterior-posterior axis in the anterior wing (Figure 3G, 7) [91]. When Fat signaling is disrupted by viable mutations, or RNAi of *ds* or *fat*, or in Wts-rescued *fat* mutants, then ridge orientation in the posterior wing is altered such that they now run in an anterior-posterior direction (Figure 7B, C, K) [90]. In *fat* mutants expressing Fat:Fat4 and Wts, ridge runs an intermediate angle between fat RNAi and *fat* mutants expressing WT Fat and Wts, indicating partial ridge polarity activity (Figure 7H, K).

The observation that Fat:Fat4 could largely rescue the *fat* PCP phenotype, but not growth deficiency (Figure 1C, G, J, K-N), implies that the Fat-PCP signal transduction mechanisms are conserved from *Drosophila* to humans, and they rely on shared structural motifs.

Identification of motifs required for distinct Fat signaling pathways

The majority of sequence similarity between the *Drosophila* Fat and human Fat4 ICDs falls in 6 clusters of sequence identity (annotated ΔA through ΔF, Figure 2A, 8). To assess the functional significance of these conserved domains, we deleted them one at a time in ICD of the genomic *fat* construct. We also applied the same strategy to study the

function of EGF domains of Fat, in which all four EGF domains in *fat* ECD were deleted (Figure 9B).

These 7 mutant *fat* constructs were transformed to the same chromosome location as the wild-type *Drosophila fat* transgene (attP2 at 68A4), and none of them exhibited any dominant phenotype in wild-type *fat* background (Data not shown). Then these mutant fat transgenes are crossed into *fat* null mutant backgrounds. The expression levels of these modified Fat transgene in *fat* null mutant were examined by subjecting 3rd instar larvae wing discs lysates to Western blotting, and are comparable to that of endogenous *fat* gene (Figure 4M).

In *fat* null mutant backgrounds, only FatΔEGF fails to rescue the lethality of *fat* null mutant (Figure 1D), and give overgrown wing discs (Figure 9G), while all six of the ICD deletions rescued lethality. When lethality is rescued by overexpression of Wts, *fat* mutant with FatΔEGF behaves indistinguishable from *fat* mutant for all kinds of PCP phenotypes descripted above (Figure 1D, K-N; 10A, K; 11G).

Fat mutant expressing any of the six ICD deletions could rescue lethality. To examine the significance of each motif contributing to Fat-Hippo activity, adult male wing areas were measured, and compared with those wings rescued by wild-type fat transgene (Figure 2V).

For all the assays descripted above, FatΔA, FatΔB and FatΔC rescue both the growth and PCP defect in *fat* null mutant (Figure 2C-E, V, W; 3J, K, L; 10D, E, M, N; 11D, E). The morphology of wings from these genotypes was similar to that from wild-type Fat transgene, implying that despite their evolutionary conservation, these motifs are not

essential. Conversely, animals rescued by constructs containing the other three deletions exhibited phenotypes which indicate that they provide only partial Fat activity.

FatΔD rescued *fat* mutants have an obvious increase in wing area by 29% than wild-type Fat (Figure 2F, V), indicating partially impaired Fat-Hippo activity. These animals have slightly reduced cross-vein spacing to 73% of wild type (Figure 2F, W), but obviously wilder than Wts-rescued *fat* mutants(13% of wild type, Figure 1A & data not shown). FatΔD also fails to rescue the ridge orientation (Figure 3H). However, FatΔD substantially rescue hair polarity in both wing blade (only 20% have weak phenotype) (Figure 3B, J, K) and abdomen (normal hair polarity) (Figure 3E, L), indicating FatΔD retains most PCP activity.

FatΔE rescued *fat* mutants lead to a slight increase of wing area (by 8%, Figure 2G, V), and the cross-vein spacing is 87% of wild type (Figure 2W). Nevertheless, all the other PCP phenotypes examined were fully rescued to wild-type level (Figure 3D, J-L; 10F, O; 11F).

FatΔF rescued *fat* mutants cause a 4% increase of wing areas (Figure 2H, V), suggesting it has almost normal Fat-Hippo signal activity. However, the wings are shorter and wider than normal wings (12% rounder than wild-type, Figure 2H), suggesting a PCP defect, because the shape of the wing is influenced by oriented cell divisions and rearrangements. FatΔF rescued *fat* mutants shows strong PCP defects in all the assays: The cross-vein distance is substantially reduced (only 27% of wild type, compared with 13% in Wts rescued *fat* mutants) (Figure 2W). Wing hair polarity is disrupted: In the wing blade, only 38% wings have normal hair orientation while 16% exhibit strong PCP phenotype (Figure 3C, J). As the most proximal part of the anterior wing, the costa, was

affected more severely than the wing blade, we scored these regions separately. Within the costa, most FatΔF rescued wings exhibit a strong PCP phenotype (Figure 3C, K). A mild phenotype of abdomen hair polarity was observed (Figure 3F, L), which is fully rescued by other ICD transgenes. And FatΔF failed to rescue the ridge orientation (Figure 3I). Thus, FatΔF have largely normal Fat-Hippo activity whereas the Fat-PCP activity is substantially impaired.

The observation that some altered *fat* transgenes are preferentially deficient in a subset of Fat signaling activities, while retaining relatively normal activity in others, implies that Fat signals through distinct downstream pathways, which diverge at the level of Fat itself. As a genetic test of this, we performed complementation tests. The results of these experiments were consistent with the hypothesis of separable Fat activities. As expected, mutations that impair different Fat activity could complement each other. FatΔF/FatΔD could rescue both the overgrowth and PCP phenotype (Figure 2V, W; 3J, K, L). Adult wings were 7% larger than wings rescued by wild-type transgenes, which is much smaller than FatΔD rescued wings (29%) and comparable to those from FatΔF rescued wings (4%) (Figure 2I, D, H). And FatΔD provided substantial rescue of the PCP phenotypes of FatΔF (cross-vein spacing 62% of wild-type, and hair polarity rescued; Figs 2W; 3J-L; 10P). Conversely, mutations that impair the same Fat activity could complement: Fat:Fat4 fail to rescue the overgrowth of FatΔD expressing wings (33% larger than wild-type; Figure 2J, V), but did partially rescue the cross-vein spacing defect (66% of wild-type, Figure 2K, W) and hair polarity phenotypes of FatΔF (Figure 3J, K, L; 10R). This complementation is not due to dosage effect, since FatΔD/FatΔD and FatΔF/FatΔF have similar phenotype as corresponding one copy transgene (Figure 2N, O, V, W). None of

FatΔD, FatΔF or Fat:Fat4 has dominant-negative effect, since they are rescued to normal when combined with wild-type Fat+ (Figure 2L, M, P, V, W; Data not shown). Recent reports show that over-expression of Fat construct lacking the intracellular domain could provide some Fat-PCP activity in *fat* mutant, but not in *ds fat* double mutant [92, 93], presumably due to an ability of the extracellular domain of Fat to interact with Ds, and an ability of Ds to influence PCP independently of the Fat ICD. To evaluate whether this is the case under endogenous expression conditions, a Fat isoform missing the ICD within *fat* genomic rescue construct (named as FatΔICD) was analyzed (Figure 9B). This FatΔICD can't rescue the lethality of *fat* null mutant, and have overgrown wing discs typical of *fat* mutant (Figure 9H). But FatΔICD do provide partial PCP activity when lethality is rescued by overexpression of Wts. Cross-vein spacing can only be roughly estimated when Fat-Hippo activity is severely compromised, because the cross-veins are often incomplete (Figure 9I). Nonetheless, FatΔICD expressing *fat* mutant have intermediate cross-vein spacing value of 0.32, higher than *fat* mutant with Wts (0.13) and FatΔF (0.23 with Wts and 0.27 without Wts). Thus it show a weaker PCP phenotypes than *fat* null mutant (Figure 1K, L, N).It also partially rescue the wing and abdomen hair polarity phenotypes (Figure 10B, L), providing more Fat-PCP activity than FatΔEGF, but less than Fat:Fat4 or FatΔF.

Influence of deletion mutations on Fat protein levels, localization, and phosphorylation

To investigate the underlying molecular mechanism for effects on Fat activity, we examine the localization, levels, and potential modifications of these mutant Fat proteins. Immunostaining in wing discs against Fat protein shows that all six of the ICD deletions

appear to be expressed at normal levels and localized normally to the sub-apical membrane (Figure 4 & Data not shown). Conversely, FatΔEGF was expressed, but localized within the cytoplasm, and fail to accumulate at the normal sub-apical membrane location (Figure 4B, E). This miss-folding and mis-localization may explain why FatΔEGF can't provide any detectable Fat activity in our assays. Western blotting of wing disc lysates from different transgene gives comparable Fat protein level (Figure 4M).

Although the ICD deletions localize normally, western blotting revealed an intriguing effect of the ΔD mutation on Fat protein mobility. In wild type, Fat is cleavage to yield several fragments [46, 47]. Among which a 95kD fragment runs as smeared doublet in western blotting and the reduced mobility of the upper band depends on phosphorylation. In *dco*^{3} or *ds* mutants, the relative fraction of the 95kD fragment that appeared in the upper band was reduced and the fraction in the lower band was increased, suggesting a correlation between phosphorylation and Fat-Hippo activity. Intriguingly, in *fat* mutant expressing FatΔD, which largely impairs Fat-Hippo activity, a similar change on 95kD fragment mobility was observed (Figure 4M, N): the relative fraction of the 95kD product that appeared in the upper band was reduced and the fraction in the lower band was increased (Figure 4M lane 5), mimicking the influence of *dco*^{3} or *ds* mutants on Fat mobility (Figure 4N lane5). Otherwise, the other Fat deletions with almost normal Fat-Hippo activity (FatΔA, FatΔB, FatΔC, FatΔE, and FatΔF) show smeared doublet not distinguishable from wild type (Figure 4M).

Identification of Dco phosphorylation sites

Independent from the analysis of conserved sequence motifs, we took advantage of the correlation between Fat phosphorylation and Fat-Hippo signaling, to identify the Dco phosphorylation site on Fat. As a similar Dco-dependent mobility shift of Fat is detected both in vivo and in cultured cells [46, 47], we first used a cultured cell assay. Fat constructs containing deletions of parts of the ICD (Figure 5A; 13) was co-expressed with Dco or a mutant isoform that fails to phosphorylate Fat (Dco^3), and S2 cell lysates were subjected to Western blotting to test the mobility of corresponding Fat polypeptide. A Fat polypeptide containing amino acids 172 through 415 of the ICD (ft-STI-11:FVH) was shifted by co-expression with Dco, whereas constructs encompassing further deletions of this region were not affected (Figure 5A). This observation suggested that either recognition by Dco, or the ability to detect a mobility shift, was lost when this region (ft-STI-11:FVH) was further truncated. Then we turned to site-specific mutagenesis to further pinpoint the exact amino acids required for Dco phosphorylation on Fat. Amongst a series of 20 different constructs (P1 to P20) with clusters of potential phosphorylation sites within this region mutated (Figure 13), the mobility shift of eighteen constructs appeared normal, whereas that of P14 and P15 was impaired (Figure 5B; 12A, B). The 10 Ser residues affected by P14 or P15 were then changed to Ala alone and in combinations within 13 additional constructs (P21 to P33, Figure 13). This identified three Ser residues as contributing to the Dco-dependent mobility shift (Figure 5B; 12). When any of these were individually mutated to Ala (P25, P26, P27, Figure 13), the mobility shift was reduced, and when all three were changed to Ala (P32) the mobility shift was eliminated (Figure 5B). Introduction of a phosphomimetic residue, aspartic acid, into these sites (P15D, P32D, Figure 13) was sufficient to introduce a modest, Dco-independent, mobility shift (Figure 12B).

However, when the P15, P15D, P32 or P32D amino acid substitutions were introduced into Fat genomic construct (P32, Figure 13), the resulting mutant transgene could provide almost full Fat activity (Figure 2Q, V, W; 3J, K, L; 10C), besides a negligible effect on wing hair polarity (Figure 3J; 10C). Although the mobility shift of Ft-95 fragment is still impaired in the fat mutant expressing P32 (Figure 4N; 5B; 12C), these phosphorylation sites are not essential for Fat activity transduction. To reconcile this with the evidence that Dco-dependent phosphorylation is linked to Fat activity, We hypothesize there might be multiple Dco sites on Fat, some of which are required for signal transduction but don't visibly influence Fat mobility, while others are required for visible mobility shift but not signal transduction. Thus we recruit more sophisticated strategy to investigate this question. My colleague Gongping Sun made additional Fat genomic constructs, in each of them a cluster of six to ten Ser and Thr residues were changed to Ala by mutagenesis (Fat-mI, Fat-mIV, and Fat-mV. Figure 2A; 8). They are recombineered into *fat* genomic constructs and transformed. None of them exhibit any dominant phenotype. They were crossed into *fat* null mutant background and subjected to the same assays as the ICD deletions. Fat-mIV has virtually normal Fat activity, as it could rescue both growth and PCP phenotype of *fat* mutant pretty well, only a negligible wing hair polarity defects were observed (Figure 2R, V, W; 3J, K, L; 10H).

fat mutant with Fat-mI exhibits a moderate increase of wing area (by 18%, Figure 2S, V). And the cross-vein spacing is 77% of wild-type (Figure 2W), a weak hair polarity defect was found in wing blade, but normal in costa or abdomen (Figure 3J, K, L; 10G). This region overlaps with a part of the Fat ICD identified by Matakatsu et al [93] as important for Hippo signaling (Figure 2A). One curious feature of Fat-mI is that it actually

decreases the mobility of Fat ICD (Figure 4N), since the fraction of upper band increase at the expense of lower band for Ft-95. This interesting phenotype supports our hypothesis that Fat mobility requires sites other than those essential for signal transduction.

Fat-mV, whose point mutations span a region overlaps the region deleted in FatΔD (Figure 2A; 8), exhibits phenotypes similar to FatΔD in all respects: similar extent of over-growth (35% for Fat-mV in and 29% for FatΔD, Figure 2T, V); Similar cross-vein spacing (79% and 73%, Figure 2W) and weak hair polarity phenotypes (Figure 3J, K, L; 10I, Q); Fat-mV localizes to normal sub-apical membrane (Figure 4I,L). *fat* mutant with Fat-mV has reduced phosphorylation of Ft-95 in a manner similar to that of FatΔD (Figure 4N), implicating these residues as essential Fat phosphorylation site(s) in vivo. This region also overlaps with the previously identified Dco binding site (Figure 2A) [47], thus I investigate the possibility that ΔD or mV might indirectly affect Fat signal activity by reducing Dco binding affinity. However, introduction of ΔD or mV into a UAS-ftICD (ft-STI:FVH) construct doesn't affect its ability to bind Dco in cultured S2 cell (Figure 5C). Thus, these sites are required for Fat-Hippo signaling and Fat ICD phosphorylation.

Influence of Fat mutations on Dachs localization

The correlation of Dachs localization with Fat activity implicates Dachs regulation as a key step in Fat signaling, but how it transduce Fat-Hippo and Fat-PCP signaling differentially is unclear. To investigate whether different Fat activity from ICD mutations is correlated with Dachs localization, we made clones of cells expressing a tagged Dachs isoform (Dachs:Cit) [39] in *fat* mutant wing discs expressing FatΔD, FatΔF, and

Fat:FAT4, and examined the localization of Dachs:Cit in the clones. When induced at appreciate developing stage and frequency, these Dachs:Cit clones serve as a powerful tool to reveal the localization of Dachs.

Dachs:Cit normally localizes on membranes on distal side of the clone in wild type discs; while in *fat* null mutant discs, Dachs accumulates to the membrane all around the entire circumference of the clone (Figure 6E,K). Wild-type *fat* genomic transgene could rescue the Dachs polarization (Figure 6A, G). Fat:FAT4 and FatΔD, which impair Fat-Hippo activity but retain substantial PCP activity, exhibit an intermediate Dachs membrane localization phenotype: while some clones have normally polarized Dachs localization, some other clones has Dachs all around the circumference of clones or increased Dachs membrane localization (Figure 6B, H, D, J). FatΔF expressing wing disc showed another unique profile: in many clones Dachs are still polarized, localize on only one side of the clone, but pointing to random directions (Figure 6C, I).

To quantify these effects, Dachs localization images collected from *fat-,* and *fat* rescued by wild-type Fat+, Fat:Fat4, FatΔD, or FatΔF transgenes were assigned random numbers and then scored together without knowledge of the genotypes. In this blind scoring, Dachs:Cit clones were first categorized as either non-polarized (Dachs localizes to the membrane around the circumference of the clone), multi-directional (Dachs localizes to the membrane around only part of a clone, but without a consistent direction of polarization), or unidirectional (Dachs is polarized in one direction). Then, amongst the unidirectional clones, the direction in which Dachs was polarized was scored. To simply this analysis, only clones in the medial 2/3 of the wing pouch were scored, as in this region the distal polarization of Dachs points towards the dorsal-ventral compartment boundary, which can be identified by

expression of Wg. In animals with Fat+ transgenes, 94% of clones were scored as unidirectional, and the vast majority of these were scored as having distally localized Dachs (Figure 6F, G). Conversely, in *fat* mutant animals, only 13% of clones were scored as unidirectional, and of these few unidirectional clones, only half were scored as having distally-localized Dachs (Figure 6F, K). Fat:Fat4- and FatΔD-rescued animals were both intermediate in terms of the fraction of clones scored as non-polarized or unidirectional (Figure 6F, H, J). FatΔF-rescued animals had a smaller fraction of "non-polarized" clones than Fat:Fat4 or FatΔD, and the largest fraction of "multidirectional" of all the genotypes (Figure 6F). Moreover, amongst the "unidirectional" clones, the direction of polarization was partially randomized (Figure 6I). These observations identify a correlation between the influence of Fat ICD mutations on Hippo or PCP signaling, and their influence on Dachs localization.

Recent studies have revealed that Fat and Ds are themselves partially polarized in wing cells [74, 76]. To investigate whether the partial randomization of polarity in FatΔF occurs at the level of Fat localization, we took advantage of the observation that the polarized localization of Fat results in an anisotropy of Fat staining along Proximal-distal (PD) interfaces as compared to anterior-posterior (AP) interfaces [74]. No difference in this anisotropy of localization was detected for a wild-type Fat construct versus FatΔF (Figure 6L), which suggests that this mutation affects downstream signal transduction rather than Fat localization.

Influence of directed Dachs membrane localization on Hippo and PCP signaling

To confirm the importance of Dachs membrane localization and distinguish it from other potential influences of Fat, we sought to localize Dachs to the membrane independently

of fat mutation. One approach for membrane targeting is to attach a peptide sequence for lipidation. However, when a myristylation signal was attached to Dachs (Myr:Dachs), rather than activating Dachs, it appeared to create a dominant negative protein, as expression of Myr:Dachs phenocopied dachs mutations (Figure 7E, P). Dachs normally has very discrete localization at the sub-apical membrane, near E-cadherin, whereas Myr:Dachs is broadly localized on membranes throughout the cell (Figure 7G,H). Thus, we sought an alternative approach that would target Dachs to the correct location. Studies of Zyx identified it as a component of the Fat-Hippo pathway, and suggested a model in which Dachs acts at the membrane in association with Zyx [60]. Thus, we constructed a Zyx:Dachs fusion protein, expressed under UAS control. This fusion protein exhibited a Zyx-like localization profile, as it localized to the sub-apical membrane around the entire circumference of the cell, rather than exhibiting the polarized localization characteristic of Dachs (Figure 7I, J). When expressed in the developing wing under nub-Gal4 control, it resulted in a strong wing overgrowth phenotype (Figure 7F), and like reductions of *fat* it decreased Warts levels (Figure 7K). These overgrown wings did not flatten properly, and hence it was difficult to compare their size with wings co-expressing wild-type forms of Zyx and Dachs, which also overgrow (Figure 7D), but Zyx:Dachs-expressing wings nonetheless appeared to be slightly larger. A stronger activation of Yki was also evident when comparing wing discs expressing the Zyx;Dachs fusion protein to wing discs co-expressing Zyx and Dachs: the discs became more highly folded, which can be a consequence of overgrowth, and a Yki target gene, ex-lacZ, was highly expressed (Figure 7Q). The consequences of fusing Zyx and Dachs was even more dramatic when PCP was examined, as co-over-expression of

Zyx and Dachs does not have significant effects on hair polarity (Figure 7S), but expression of Zyx:Dachs resulted in a strong disturbance of wing hair polarity (Figure 7T). Thus, targeting Dachs to the membrane by fusing it with Zyx phenocopies both Hippo and PCP phenotypes of *fat* mutants.

DISCUSSION

Distinct regions of Fat required for Hippo and PCP signaling

Our results indicate that effects of Fat on wing growth versus PCP can be separated at the level of Fat itself: a four amino acid deletion at the C-terminus of Fat (FatΔF) impairs PCP, but does not affect wing growth, whereas deletion or point mutations within the D motif (FatΔD, Fat-mV) result in wing overgrowth, but have weaker effects than FatΔF on PCP. Matakatsu and Blair also recently reported that they could separate regions of Fat required for Hippo and PCP activities, but identified completely different regions [93].

Matakatsu and Blair used UAS-driven expression, whereas we used genomic constructs. Because these large constructs are more difficult to manipulate, we did not undertake a comprehensive analysis of the entire ICD, but focused on candidate regions predicted from evolutionary conservation. However, our approach had the advantage that expression under endogenous conditions could identify activities that are missed when proteins are over-expressed. Thus, we observed wing overgrowth when region D was mutated, but this region was not identified by Matakatsu and Blair. Nonetheless, the ΔD and m-V mutations only partially impair Fat-Hippo activity, as they rescue the lethality of *fat* mutants, and additional Hippo activity is presumably provided by regions identified by Matakatsu and Blair [93], which are not conserved in Fat4. Hence, our combined studies imply that multiple regions of the Fat ICD contribute to Fat-Hippo signaling.

PCP was first recognized for its effects on the orientation of hairs on the body of the fly, but is now understood to encompass a wider range of cellular polarization. Matakatsu and Blair only examined hair polarity in their assessments of PCP, whereas we also considered Dachs polarization, ridge orientation, and cross-vein spacing (because cross-vein spacing is also

reduced by Fat over-expression, it could not be assessed by their approach). Outside of the costa, deletion of the F region had only minor effects on hair polarity. Instead, the PCP phenotypes of FatΔF were most noticeable when cross-vein spacing, Dachs localization, and ridge orientation were examined. Thus, the assignment of PCP activity to distinct regions of the Fat ICD by our studies does not represent a disagreement, but rather emphasizes that there are different types of PCP, which can be genetically separated.

Analysis of PCP phenotypes for Fat constructs that do not rescue lethality depends upon Wts over-expression. The wing hair PCP phenotype of these animals is restricted to the proximal wing. Moreover, they have strong disruptions of abdominal PCP, but typically only part of each abdominal segment is affected. Indeed, the hair phenotype of Wts-rescued *fat* mutants appear to us similar to that described for *fat* mutants rescued by the Fat ICD-only expressing construct fatICD, which has been interpreted as a partial rescue of hair polarity [93]. We suggest, therefore, that some of the hair PCP phenotype ascribed to *fat* could reflect effects on transcription of downstream target genes, mediated via downregulation of Wts. Our results also support the conclusion that some of the influence of Fat on PCP reflects an activity of the ECD as a ligand for Ds, indicating that Ds-Fat PCP signaling is bidirectional, with Fat and Ds acting as both receptor and ligand for each other. Previous experiments showed that when over-expressed, the Fat ECD could influence PCP in a Ds-dependent fashion [93, 94]; we have now confirmed that FatΔICD partially rescues *fat* PCP phenotypes even at endogenous expression levels.

A conserved motif required for Fat PCP signaling

Fat4 and *Dchs1* mutant mice have phenotypes that are consistent with effects on PCP [31, 81], but the molecular mechanisms involved are unknown. The ability of Fat:Fat4 to rescue

fat PCP phenotypes indicates that there are conserved mechanisms of Fat-PCP signaling involving the Fat ICD. Amongst conserved sequence motifs, the four amino acid "F" motif is clearly required for PCP, which implicates it as being involved in a conserved PCP mechanism. These four amino acids resemble a PDZ domain binding motif, which suggests that it might interact with a PDZ domain-containing protein.

A striking feature of FatΔF rescued *fat* mutants is the partial randomization of Dachs polarization. The observation that Dachs can be polarized, but in a variable direction, suggests that there are multiple steps involved in establishing Dachs polarization, i.e. control over whether Dachs localization is polarized can be mechanistically uncoupled from control over the direction in which Dachs is polarized.

Role of Dachs localization in Fat signaling

The observation of both randomized Dachs localization and rounder wings with more closely spaced cross-veins in FatΔF rescued animals extends the correlation between polarized Dachs localization and PCP phenotypes, and is consistent with the hypothesis that Dachs polarization directs polarized cell behaviors. We also found a rough correlation between the decreased Fat-Hippo pathway activity of Fat:Fat4 or FatΔD, and increased detection of Dachs at the sub-apical membrane. These results are at least generally consistent with the hypothesis that the direction in which Dachs localization is polarized influences PCP, whereas the amount of Dachs on the membrane influences Hippo signaling [29, 36, 38]. These and other studies identified a correlation between Dachs localization and Fat signaling, but could not prove that altered Dachs localization is a cause rather than a consequence of Fat signal transduction, nor separate the role of Dachs localization from other potential effects of Fat. We have now directly confirmed the importance of Dachs localization by creating a

Zyx:Dachs fusion protein, the expression of which in otherwise wild-type animals phenocopies *fat* mutants both for wing growth and PCP phenotypes.

Role of Fat phosphorylation in Fat-Hippo signaling

Despite our extensive investigation of potential phosphorylation sites, the role of Fat receptor phosphorylation in signal transduction remains elusive. Fat is directly phosphorylated by Dco, which is required for Fat-Hippo signaling, and acts genetically upstream of *dachs* and *Zyx* [21, 46, 47, 60]. Moreover, Fat ICD phosphorylation correlates with Fat activity in dco^3 or *ds* mutants, or with selected ICD mutations (FatΔD, Fat-mV). However, other Fat ICD mutations impair Fat phosphorylation without affecting Fat signaling (Fat-P32, Fat-P15). Moreover, dco^3 does not affect Dachs localization, but FatΔD, which impairs Fat-Hippo signaling and Fat phosphorylation, does affect Dachs localization. To reconcile these observations, we propose that Dco normally blocks the ability of Zyx and Dachs to inactivate Wts through a mechanism that is independent of the influence of Fat on Dachs localization. Fat might be the key substrate of Dco in this process, but our results are equally consistent with the possibility that phosphorylation of the Fat ICD by Dco is a consequence, not a cause, of Fat receptor activation, and thus while it can serve as a marker of Fat activity, the biologically important substrate of Dco might be some other protein.

Figures

Figure 1. Rescue of *fat* PCP phenotypes by Fat4

A-D) Adult wings from $fat^{8}/fat^{G\text{-}rv}$ expressing *tub-Gal4 UAS-wts* and B) *P[acman]V5:fat[68A4],* C) *P[acman]V5:fat:FAT4[68A4],* D) *P[acman]V5:fatΔEGF[68A4].* E-G) Proximal anterior wings from $fat^{8}/fat^{G\text{-}rv}$ expressing *tub-Gal4 UAS-wts* and F) *P[acman]V5:fat[68A4],* G) *P[acman]V5:fat:FAT4[68A4].* H-J) Abdominal segment from $fat^{8}/fat^{G\text{-}rv}$ expressing *tub-Gal4 UAS-wts* and I) *P[acman]V5:fat[68A4],* J) *P[acman]V5:fat:FAT4[68A4].* K-L) Histogram showing distribution of PCP phenotypes (according to key, M) in K) abdomen and L) proximal wing for animals of the indicated genotypes. N) Average distance between cross-veins in animals of the indicated genotypes, normalized to the value in wild-type rescued animals; error bars show sem.

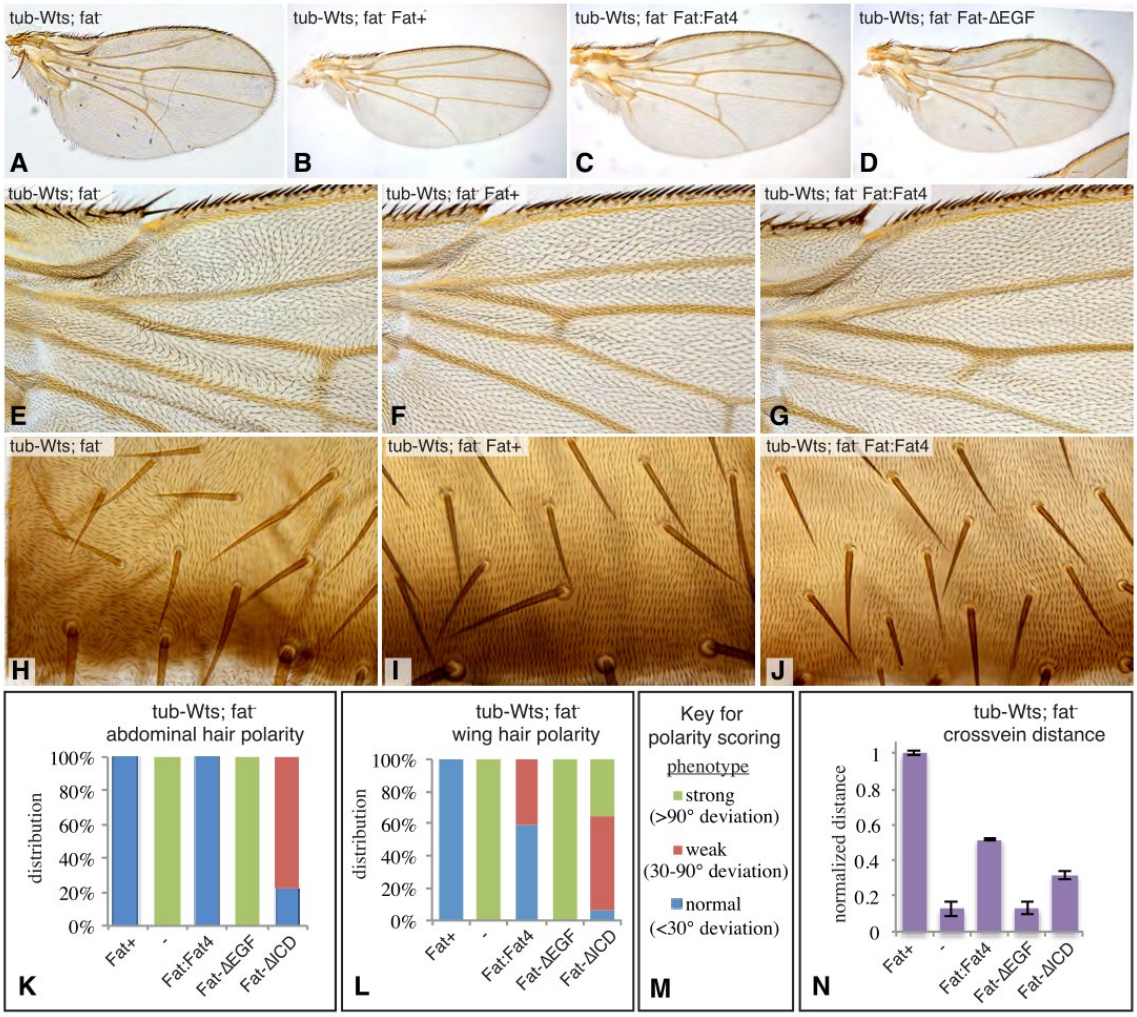
tub-Wts; fat-
tub-Wts; fat- Fat+
tub-Wts; fat- Fat:Fat4
tub-Wts; fat- Fat-ΔEGF
A
B
C
D
tub-Wts; fat-
tub-Wts; fat- Fat+
tub-Wts; fat- Fat:Fat4
E
F
G
tub-Wts; fat-
tub-Wts; fat- Fat+
tub-Wts; fat- Fat:Fat4
H
I
J
tub-Wts; fat-
abdominal hair polarity
distribution
100%
80%
60%
40%
20%
0%
Fat+
-
Fat:Fat4
Fat-ΔEGF
Fat-ΔICD
K
tub-Wts; fat-
wing hair polarity
distribution
100%
80%
60%
40%
20%
0%
Fat+
-
Fat:Fat4
Fat-ΔEGF
Fat-ΔICD
L
Key for
polarity scoring
phenotype
strong
(>90° deviation)
weak
(30-90° deviation)
normal
(<30° deviation)
M
tub-Wts; fat-
crossvein distance
normalized distance
1
0.8
0.6
0.4
0.2
0
Fat+
-
Fat:Fat4
Fat-ΔEGF
Fat-ΔICD
N

Figure 1

Figure 2. Wing phenotypes associated with Fat intracellular domain motif mutations

A) Schematic of Fat ICD with relative locations of mutations examined here (red and green bars), regions that bind Fat-associated proteins (blue bars), and functional regions identified by Matakatsu and Blair [93] (purple). B-U) Adult wings from $fat^{8}/fat^{G\text{-}rv}$ expressing B) *P[acman]V5:fat[68A4],* C) *P[acman]V5:fatΔA[68A4],* D) *P[acman]V5:fatΔB[68A4],* E) *P[acman]V5:fatΔC[68A4],* F) *P[acman]V5:fatΔD[68A4],* G) *P[acman]V5:fatΔE[68A4],* H) *P[acman]V5:fatΔF[68A4],* I) *P[acman]V5:fatΔD[68A4]/ P[acman]V5:fatΔF[68A4],* J) *P[acman]V5:fatΔD[68A4]/ P[acman]V5:fat:FAT4[68A4],* K) *P[acman]V5:fatΔF[68A4]/ P[acman]V5:fat:FAT4 [68A4],* L) *P[acman]V5:fat[68A4]/ P[acman]V5:fatΔD[68A4],* M) *P[acman]V5:fat[68A4]/ P[acman]V5:fatΔF[68A4],* N) *P[acman]V5:fatΔF[68A4]/ P[acman]V5:fatΔF[68A4],* O) *P[acman]V5:fatΔD[68A4]/ P[acman]V5:fatΔD[68A4],* P) *P[acman]V5:fat[68A4]/ P[acman]V5:fat:FAT4[68A4],* Q) *P[acman]V5:fat-P32[68A4],* R) *P[acman]V5:fat-mIV[68A4],* S) *P[acman]V5:fat-mI[68A4],* T) *P[acman]V5:fat-mV[68A4],* U) *P[acman]V5:fatΔD[68A4]/ P[acman]V5:fat-mV[68A4].* V) Average wing size in animals of the indicated genotypes, normalized to the value in wild-type rescued animals; error bars show sem. W) Average distance between cross-veins in animals of the indicated genotypes, normalized to the value in wild-type rescued animals; error bars show sem. Additional statistics on wing measurements are in Supplementary Table S1.

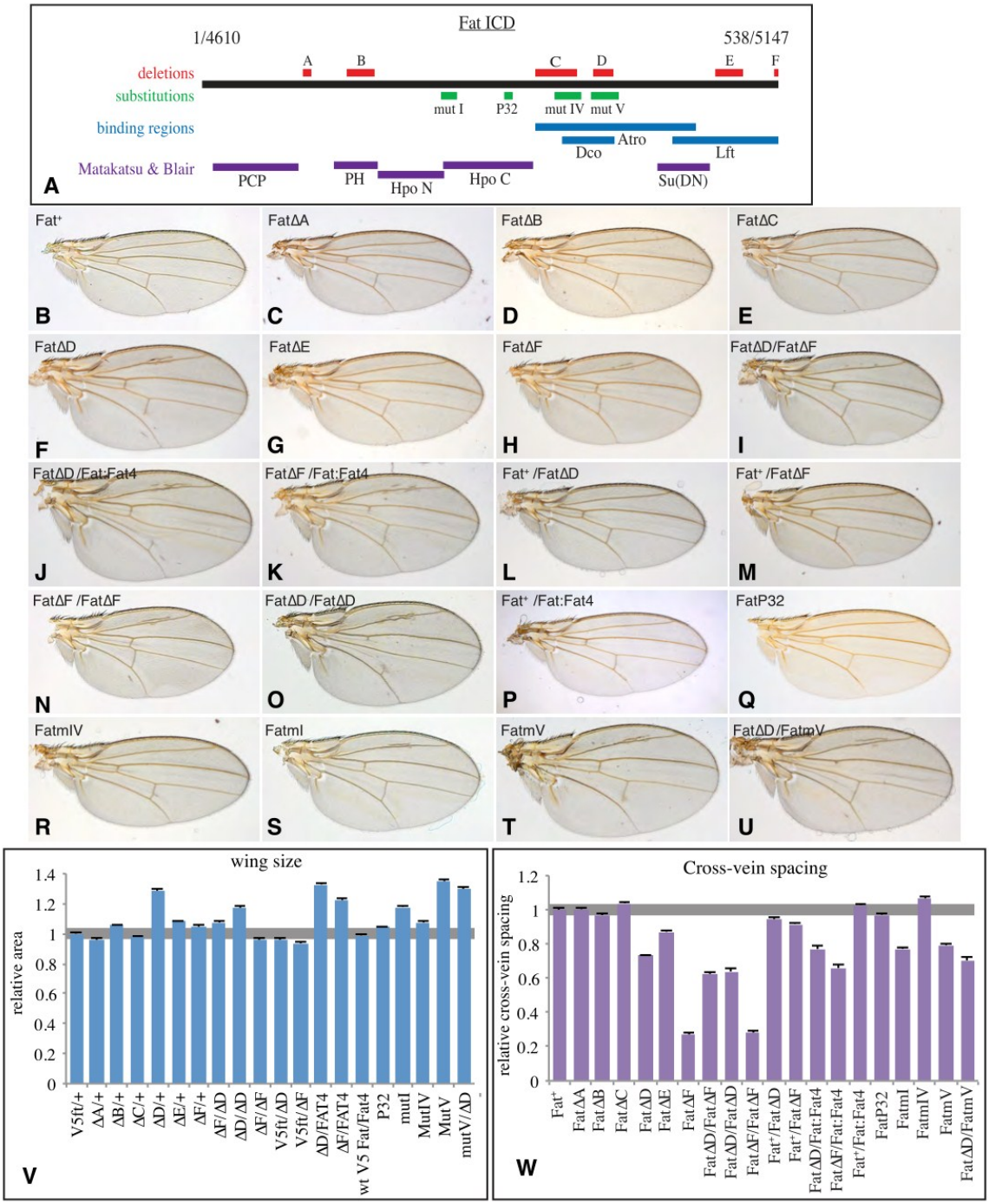
Fat ICD
1/4610
538/5147
A
B
C
D
E
F
deletions
substitutions
mut I
P32
mut IV
mut V
binding regions
Atro
Dco
Lft
Matakatsu & Blair
PCP
PH
Hpo N
Hpo C
Su(DN)
A
Fat+
FatΔA
FatΔB
FatΔC
FatΔD
FatΔE
FatΔF
FatΔD/FatΔF
FatΔD /Fat:Fat4
FatΔF /Fat:Fat4
Fat+ /FatΔD
Fat+ /FatΔF
FatΔF /FatΔF
FatΔD /FatΔD
Fat+ /Fat:Fat4
FatP32
FatmIV
FatmI
FatmV
FatΔD/FatmV
wing size
relative area
1.4
1.2
1
0.8
0.6
0.4
0.2
0
V5ft/+
ΔA/+
ΔB/+
ΔC/+
ΔD/+
ΔE/+
ΔF/+
ΔF/ΔD
ΔD/ΔD
ΔF/ΔF
V5ft/ΔD
V5ft/ΔF
ΔD/FAT4
ΔF/FAT4
wt V5 Fat/Fat4
P32
mutI
MutIV
MutV
mutV/ΔD
V
Cross-vein spacing
relative cross-vein spacing
1.2
1
0.8
0.6
0.4
0.2
0
Fat+
FatΔA
FatΔB
FatΔC
FatΔD
FatΔE
FatΔF
FatΔD/FatΔF
FatΔD/FatΔD
FatΔF/FatΔF
Fat+/FatΔD
Fat+/FatΔF
FatΔD/Fat:Fat4
FatΔF/Fat:Fat4
Fat+/Fat:Fat4
FatP32
FatmI
FatmIV
FatmV
FatΔD/FatmV
W

Figure 2

Figure 3. PCP phenotypes associated with Fat ICD motif mutations

A-C) Proximal anterior wings from $fat^{8}/fat^{G\text{-}rv}$ expressing A) *P[acman]V5:fat[68A4],* B) *P[acman]V5:fatΔD[68A4],* C) *P[acman]V5:fatΔF[68A4]*. Insets show close up of the boxed region (costa). D-F) Abdomens from $fat^{8}/fat^{G\text{-}rv}$ expressing D) *P[acman]V5:fat[68A4]ΔE,* E) *P[acman]V5:fatΔD[68A4],* F) *P[acman]V5:fatΔF[68A4]*. A-C) Proximal anterior wings, visualized by cuticle refraction microscopy [91], from $fat^{8}/fat^{G\text{-}rv}$ expressing G) *P[acman]V5:fat[68A4],* H) *P[acman]V5:fatΔD[68A4],* I) *P[acman]V5:fatΔF[68A4]*. Yellow lines indicate estimated angle of ridges relative to L4 vein. J-L) Histogram showing distribution of PCP phenotypes (according to key, Fig. 1M) in J) proximal wing, K) costa, and L) abdomen for animals of the indicated genotypes.

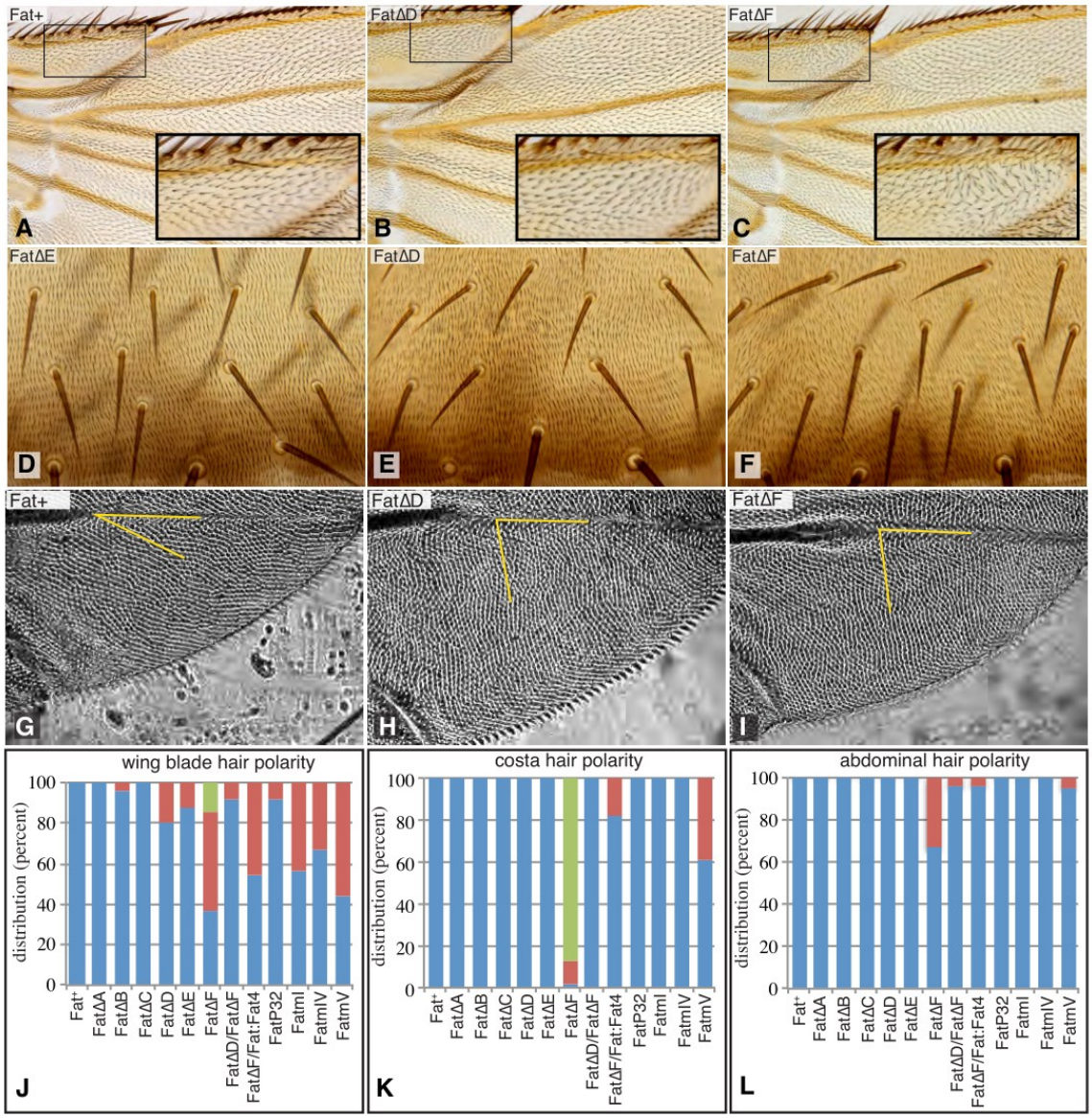
Fat+
FatΔD
FatΔF
A
B
C
FatΔE
FatΔD
FatΔF
D
E
F
Fat+
FatΔD
FatΔF
G
H
I
wing blade hair polarity
costa hair polarity
abdominal hair polarity
distribution (percent)
0
20
40
60
80
100
Fat+
FatΔA
FatΔB
FatΔC
FatΔD
FatΔE
FatΔF
FatΔD/FatΔF
FatΔF/Fat:Fat4
FatP32
FatmI
FatmIV
FatmV
J
K
L

Figure 3

Figure 4. Influence of Fat mutations on Fat protein localization and mobility

A-L) Confocal micrographs of Fat protein staining (green) in wing discs from *fat*^{8}*/fat*$^{G\text{-}rv}$ expressing A,D) *P[acman]V5:fat[68A4],* B,E) *P[acman]V5:fat*Δ*EGF[68A4],* C,F) *P[acman]V5:fat:FAT4[68A4],* G,J) *P[acman]V5:fat*Δ*D[68A4],* H,K) *P[acman]V5:fat*Δ*F[68A4],* I,L) *P[acman]V5:fat-mV[68A4].* Upper panels show horizontal sections, lower panels show vertical sections, with E-cadherin staining (red). M,N) Western blots on wing disc lysates from animals of the indicated genotypes. Upper panel shows Fat antibody staining, lower panel shows a loading control (GAPDH).

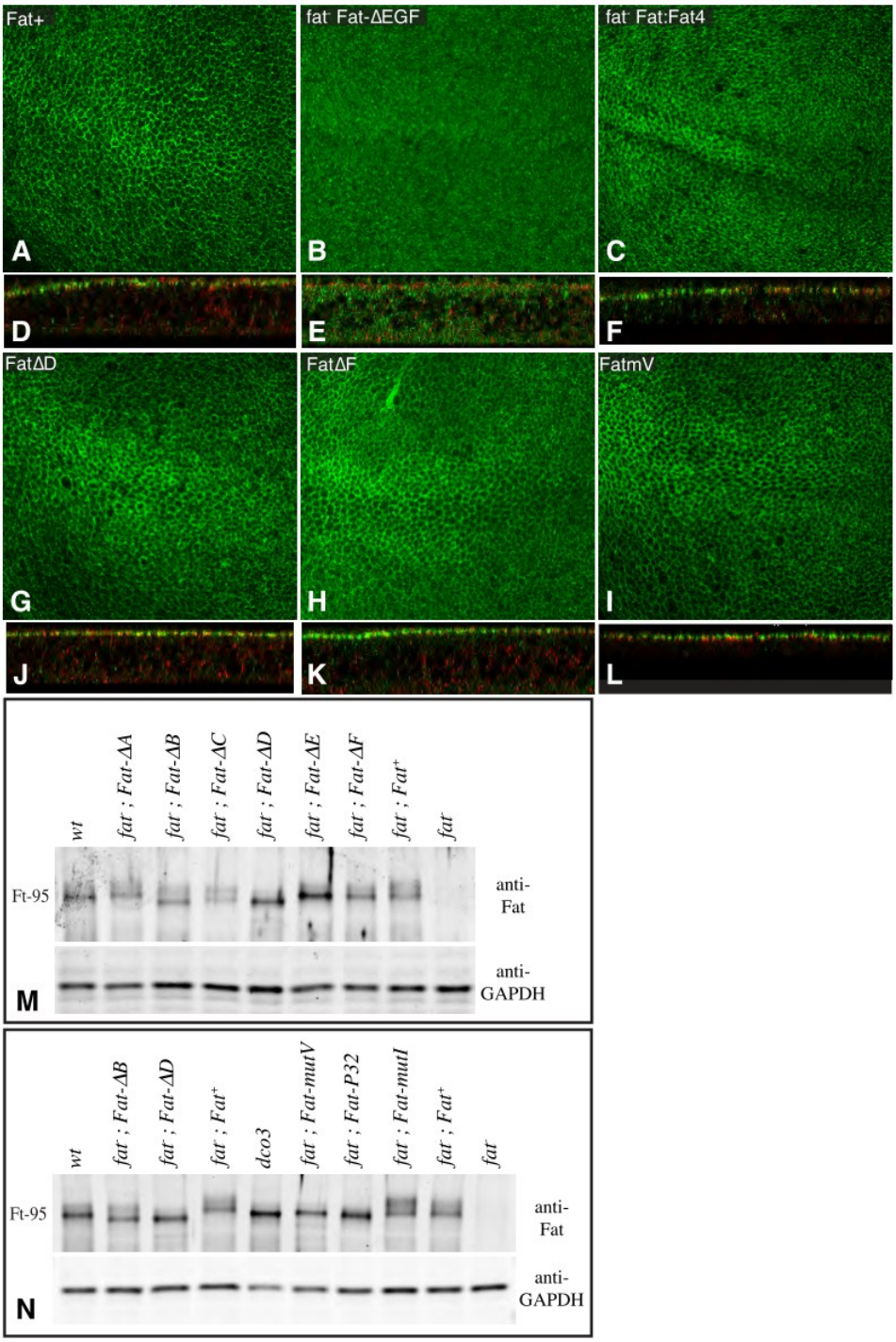
Fat+
fat⁻ Fat-ΔEGF
fat⁻ Fat:Fat4
A
B
C
D
E
F
FatΔD
FatΔF
FatmV
G
H
I
J
K
L
wt
fat⁻ ; Fat-ΔA
fat⁻ ; Fat-ΔB
fat⁻ ; Fat-ΔC
fat⁻ ; Fat-ΔD
fat⁻ ; Fat-ΔE
fat⁻ ; Fat-ΔF
fat⁻ ; Fat⁺
fat⁻
Ft-95
anti-Fat
anti-GAPDH
M
wt
fat⁻ ; Fat-ΔB
fat⁻ ; Fat-ΔD
fat⁻ ; Fat⁺
dco3
fat⁻ ; Fat-mutV
fat⁻ ; Fat-P32
fat⁻ ; Fat-mutI
fat⁻ ; Fat⁺
fat⁻
Ft-95
anti-Fat
anti-GAPDH
N

Figure 4

Figure 5. Mapping Dco phosphorylation sites in Fat

A) Fat intracellular domain truncations are indicated by dashed boxes. Portions of a blot of lysates of S2 cells expressing these constructs and Dco or Dco^3 are shown, presence of a detectable mobility shift is indicated by "+." B) Western blot on S2 cells expressing Fat-STI-4:FVH and point mutant derivatives, together with Dco or Dco^3, as indicated. The amino acids mutated are indicated in Figure S5, a D indicates a Ser to Asp mutation, in other cases Ser to Ala mutations were employed. C) Western blots showing results of co-immunoprecipitation experiments from lysates of S2 cells expressing Dco:V5 and the indicated FLAG-tagged Fat isoforms.

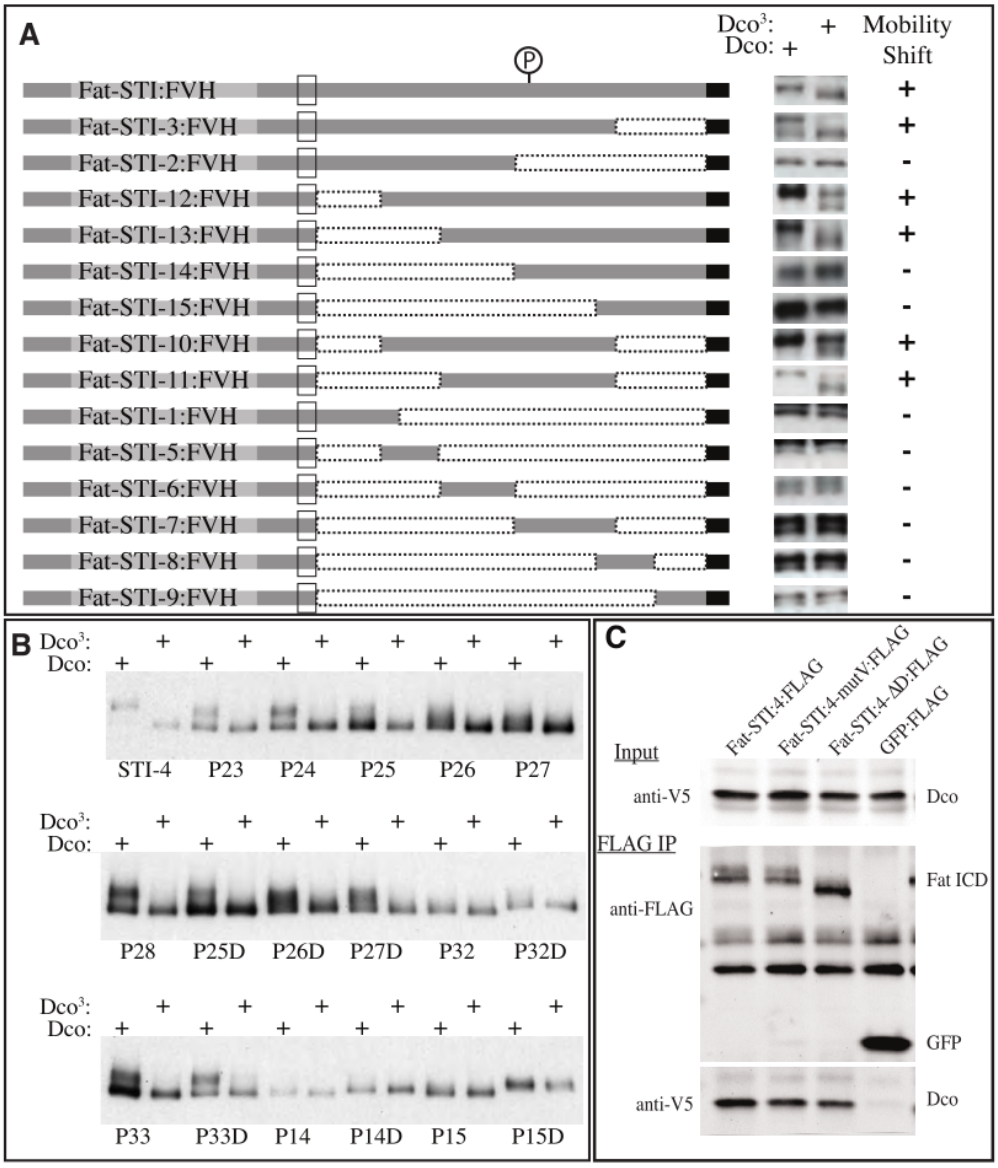
A
Dco³: +
Dco: +
Mobility Shift
Fat-STI:FVH +
Fat-STI-3:FVH +
Fat-STI-2:FVH -
Fat-STI-12:FVH +
Fat-STI-13:FVH +
Fat-STI-14:FVH -
Fat-STI-15:FVH -
Fat-STI-10:FVH +
Fat-STI-11:FVH +
Fat-STI-1:FVH -
Fat-STI-5:FVH -
Fat-STI-6:FVH -
Fat-STI-7:FVH -
Fat-STI-8:FVH -
Fat-STI-9:FVH -
B
Dco³:
Dco:
STI-4 P23 P24 P25 P26 P27
P28 P25D P26D P27D P32 P32D
P33 P33D P14 P14D P15 P15D
C
Fat-STI:4:FLAG
Fat-STI:4-mutV:FLAG
Fat-STI:4-ΔD:FLAG
GFP:FLAG
Input
anti-V5
Dco
FLAG IP
anti-FLAG
Fat ICD
GFP
anti-V5
Dco

Figure 5

Figure 6. Influence of targeted Fat mutations on Dachs localization

A-E) Examples of wing discs from animals of the indicated genotypes, with clones of cells expressing Dachs:Cit (green) from an *AyDachs:Cit* transgene. These discs are stained for expression of Wg (red, marks D-V boundary) and E-cad (blue, outlines cells). The polarity of Dachs localization is indicated by small arrows pointing in the direction of Dachs:Cit membrane localization; white arrows indicate normal polarity, yellow arrows abnormal polarity, asterisks indicate lack of polarity. Panels marked prime show the Dachs:Cit channel only from the image to the left. F) Histogram showing distribution of Dachs polarization phenotypes in animals of the indicated genotypes. Distributions were scored blind, and over 100 Dachs:Cit clones were scored per genotype. G-K) Rose plots depicting the vectors of Dachs:Cit polarization identified within polarized clones in discs of animals of the indicated genotypes. Polarities were scored blind, and the number scored is at top left. The diagrams are oriented with proximal at top, anterior at right, and distal at bottom (defined by Wg expression). Rose plots were generated using OSXStereonet, normal distal polarization is colored gray. L) Anisotropy of Fat staining along PD versus AP interfaces. NIH image J was used to calculate average staining intensities along all cell interfaces within the central region of the wing pouch, from five to six different discs, that could be defined as predominantly PD or AP based on comparison to Wg staining. Error bars indicate sem.

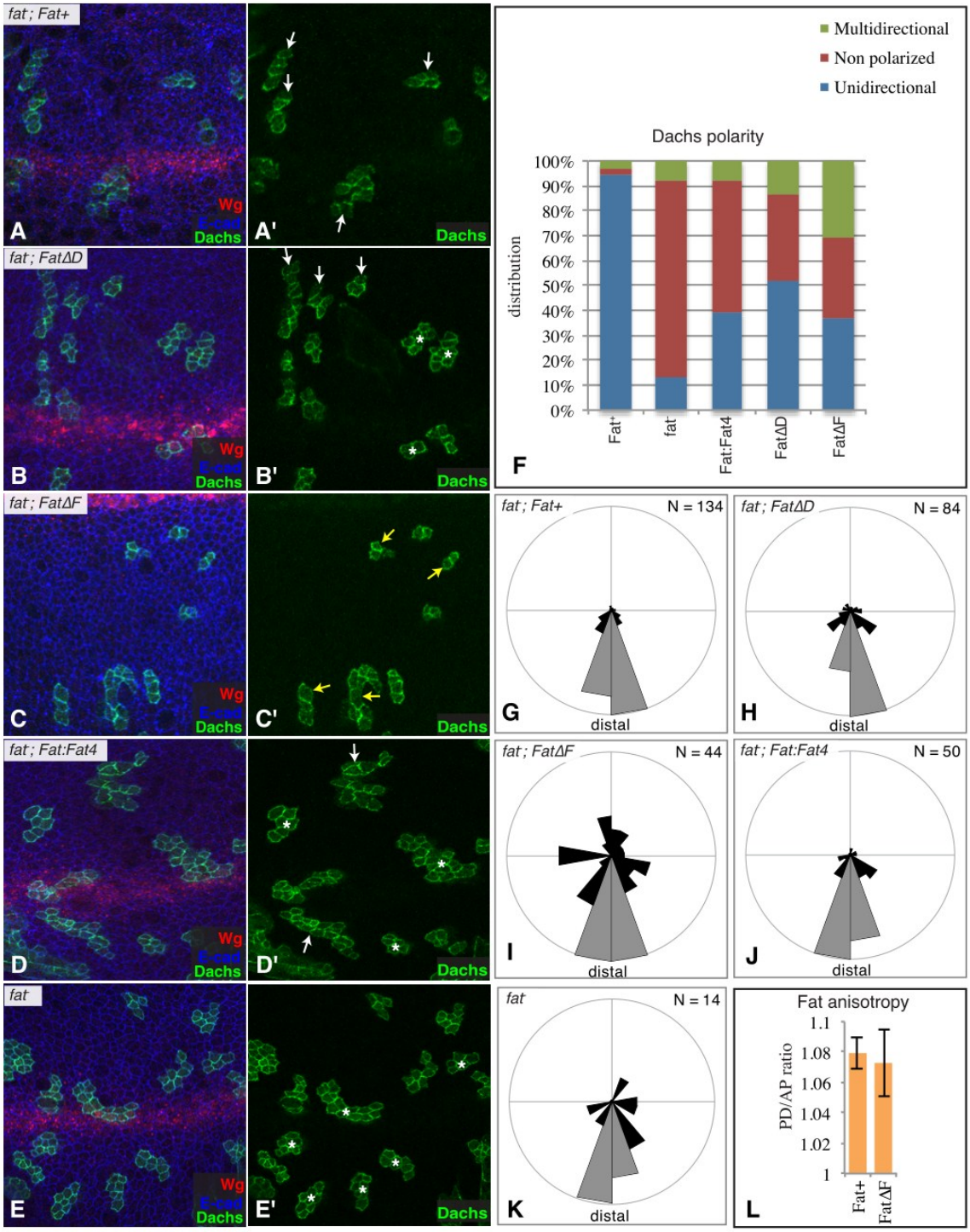
fat ; Fat+
Wg
E-cad
Dachs
A
A'
fat ; FatΔD
B
B'
fat ; FatΔF
C
C'
fat ; Fat:Fat4
D
D'
fat
E
E'
Multidirectional
Non polarized
Unidirectional
Dachs polarity
distribution
100%
90%
80%
70%
60%
50%
40%
30%
20%
10%
0%
Fat+
fat-
Fat:Fat4
FatΔD
FatΔF
F
N = 134
G
N = 84
H
N = 44
I
N = 50
J
N = 14
K
distal
Fat anisotropy
PD/AP ratio
1.1
1.08
1.06
1.04
1.02
1
L

Figure 6

Figure 7. Influence of membrane-tethered Dachs on wing growth and PCP.

A-F) Adult wings from animals expressing *nub-Gal4* and B) *UAS-Zyx*, C) *UAS-dachs*, D) *UAS-Zyx UAS-dachs*, E) *UAS-myr:dachs*, F) *UAS-Zyx:dachs*. G-J) Localization of membrane-tethered Dachs constructs. G,H) Show clones of cells expressing Myr:Dachs:V5 (green), I,J) Show clones of cells expressing Zyx:Dachs:V5 (green). G,I are horizontal sections, H,J show vertical sections.

K) Western blot on lysates of wing discs expressing *tub-Gal4* and *UAS-Dachs*, *UAS-Zyx*, *UAS-Zyx:Dachs*, or *UAS-RNAi-fat*, or mutant for *fat*, as indicated. Loss of Fat activity reduces Warts protein levels [21], GAPDH serves as a loading control. Mean Warts levels from four independent experiments, normalized to Warts levels in *fat* mutants, were: *UAS-Dachs* 3.3, *UAS-Zyx* 3.6, *UAS-Zyx:Dachs* 3.3, *UAS-RNAi-fat* 1.8, *wild type* 5.0, and *fat* mutant 1.0. L-Q) Wing discs from animals expressing *en-Gal4* (marked by *UAS-GFP*, green) and M) *UAS-Zyx*, N) *UAS-dachs*, O) *UAS-Zyx UAS-dachs*, P) *UAS-myr:dachs*, Q) *UAS-Zyx:dachs*, stained for *ex-lacZ* (red). R-T) Anterior proximal wing from animals expressing *nub-Gal4* and S) *UAS-Zyx UAS-dachs*, and T) *UAS-Zyx:dachs*.

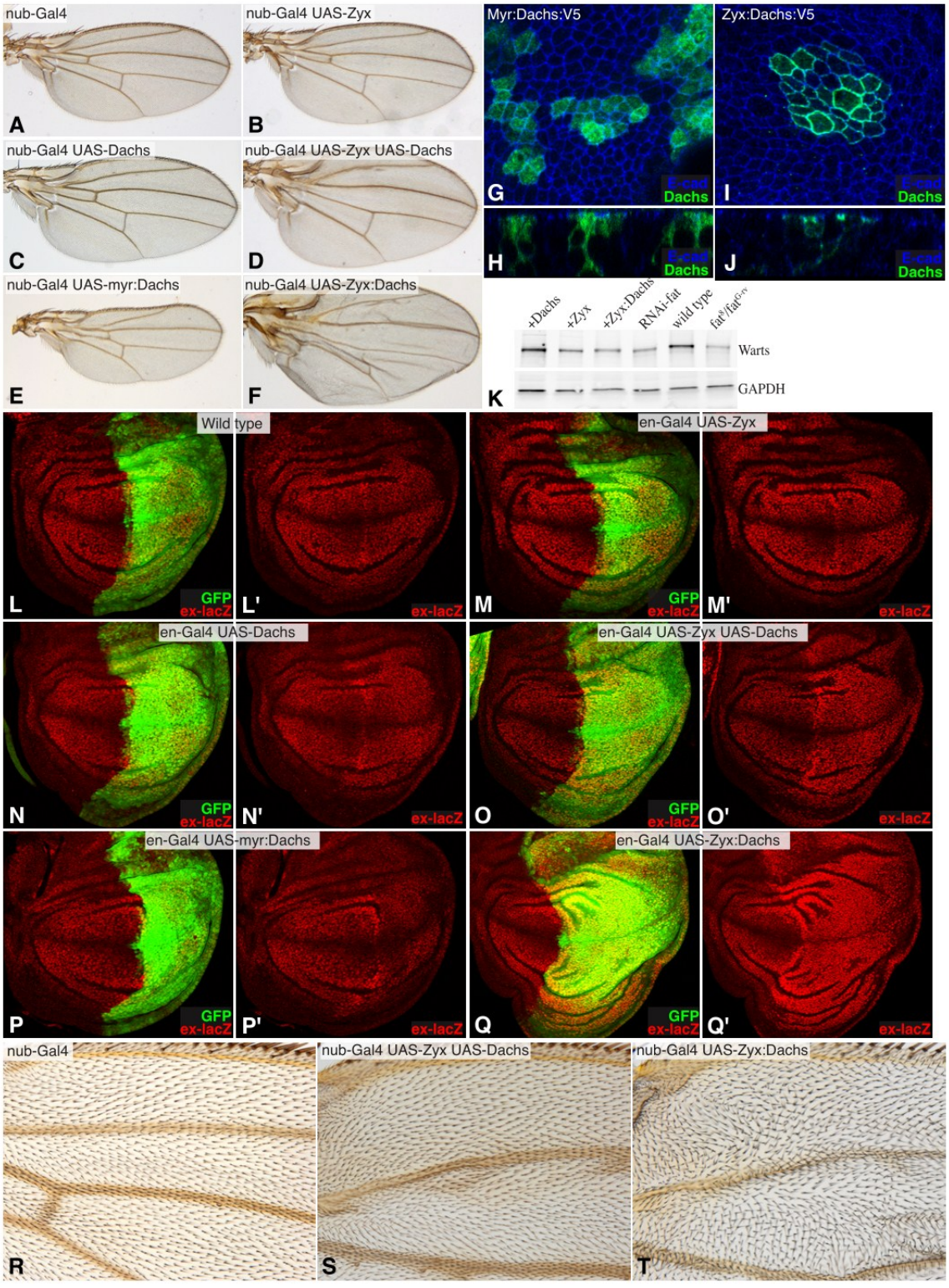
nub-Gal4
A
nub-Gal4 UAS-Zyx
B
Myr:Dachs:V5
G
E-cad
Dachs
Zyx:Dachs:V5
I
E-cad
Dachs
nub-Gal4 UAS-Dachs
C
nub-Gal4 UAS-Zyx UAS-Dachs
D
H
E-cad
Dachs
J
E-cad
Dachs
nub-Gal4 UAS-myr:Dachs
E
nub-Gal4 UAS-Zyx:Dachs
F
+Dachs
+Zyx
+Zyx:Dachs
RNAi-fat
wild type
fat8/fatG-rv
Warts
GAPDH
K
Wild type
L
GFP
ex-lacZ
L'
ex-lacZ
en-Gal4 UAS-Zyx
M
GFP
ex-lacZ
M'
ex-lacZ
en-Gal4 UAS-Dachs
N
GFP
ex-lacZ
N'
ex-lacZ
en-Gal4 UAS-Zyx UAS-Dachs
O
GFP
ex-lacZ
O'
ex-lacZ
en-Gal4 UAS-myr:Dachs
P
GFP
ex-lacZ
P'
ex-lacZ
en-Gal4 UAS-Zyx:Dachs
Q
GFP
ex-lacZ
Q'
ex-lacZ
nub-Gal4
R
nub-Gal4 UAS-Zyx UAS-Dachs
S
nub-Gal4 UAS-Zyx:Dachs
T

Figure 7

Figure 8. Alignment of Fat ICD sequences

Clustal W alignment of intracellular domains (generated at NCBI web site) of three insect Fat sequences (D.m., *Drosophila* melanogaster, T.c. Tribolium castaneum, A.m., Apis mellifera) and three vertebrate Fat4 sequences (H.s. Homo sapiens, M.m. Mus musculus, G.g. Gallus gallus). Based on transmembrane domain predictions, the ICD in D.m. Fat is 538 amino acids, and begins at amino acid 4610. Sequence identity is indicated by relative shading. Conserved motifs deleted by mutations are indicated by red lines, and regions affected by point mutations are indicated by green lines, the specific Ser and Thr residues changed in these point mutations are indicated in Fig. S5.

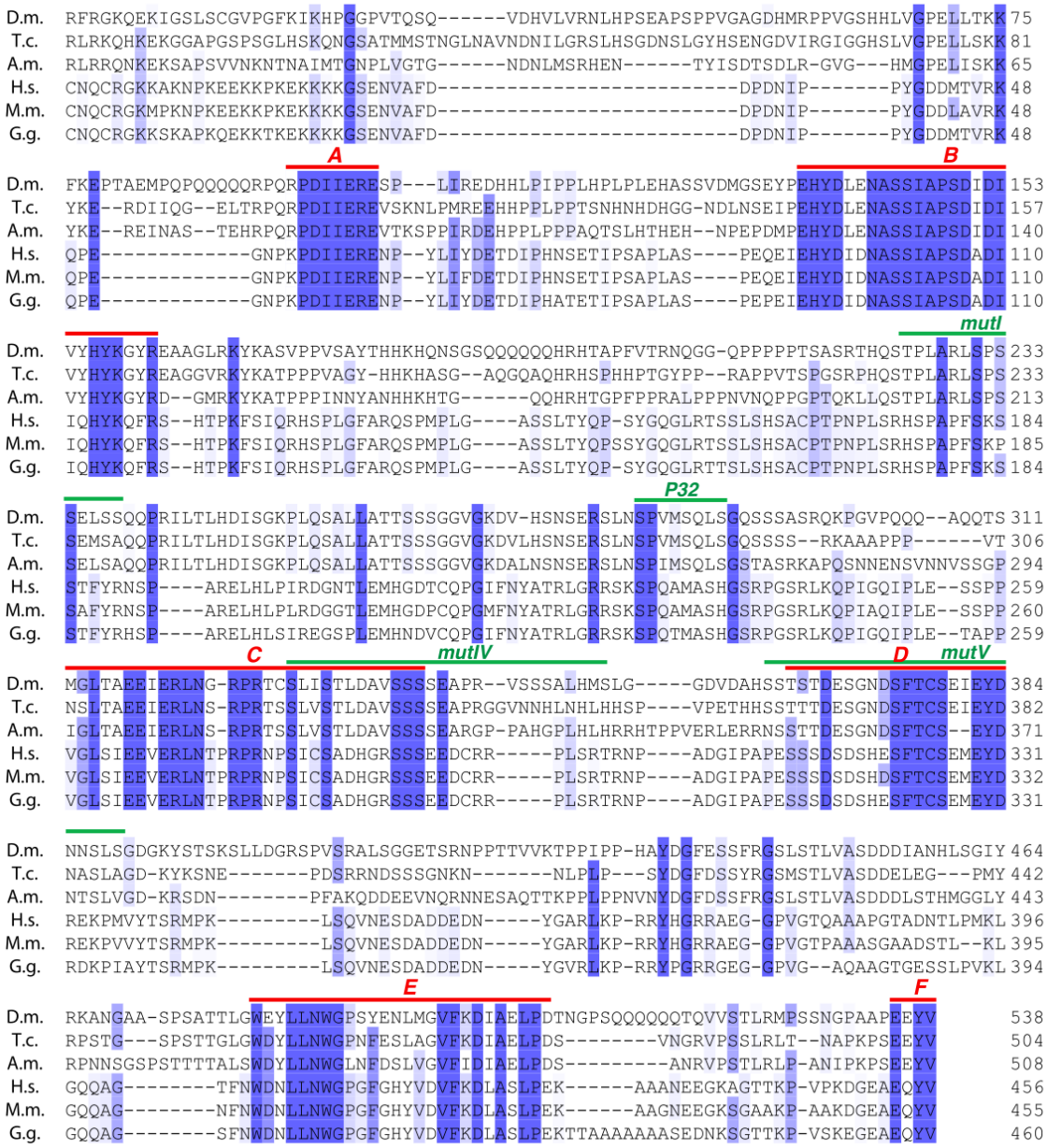

Figure 8

Figure 9. Additional analysis of Fat constructs that fail to rescue *fat* mutant lethality A) Schematic of the *fat* locus genomic rescue construct, with the region encoding the ICD highlighted in red. B) Schematics of wild-type (top) and three mutant forms of Fat examined, red indicates replacement of the *Drosophila* ICD by human Fat4 ICD. C-H) Examples of wing discs from representative late third instar larvae of the indicated genotypes, lack of Fat activity results in overgrown wing discs and increased folding in the proximal wing. I) Adult wing from $fat^{8}/fat^{G\text{-}rv}$ expressing *tub-Gal4 UAS-wts* and *P[acman]V5:fatΔICD[68A4]*.

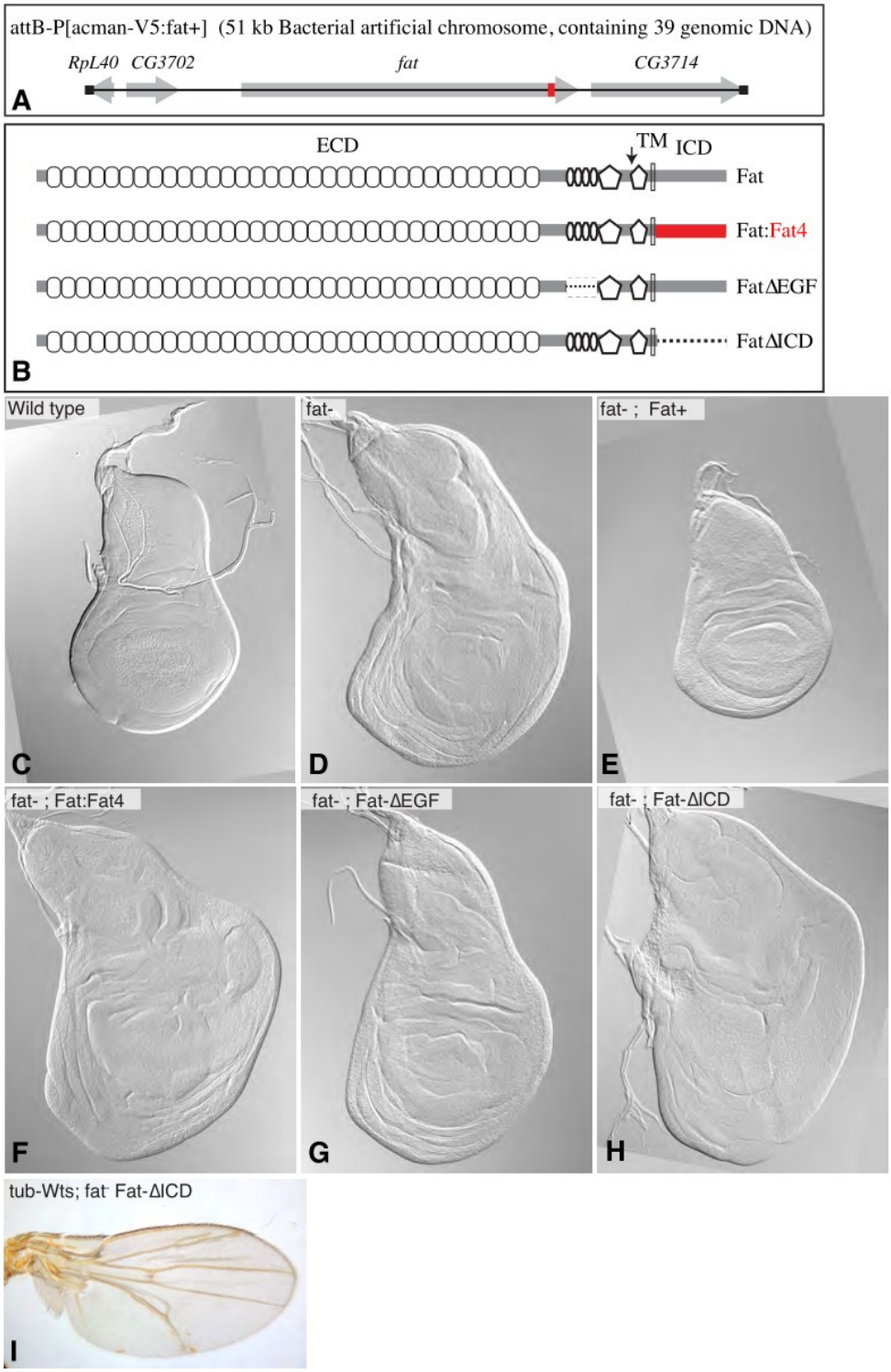
attB-P[acman-V5:fat+] (51 kb Bacterial artificial chromosome, containing 39 genomic DNA)
RpL40
CG3702
fat
CG3714
A
ECD
TM
ICD
Fat
Fat:Fat4
FatΔEGF
FatΔICD
B
Wild type
C
fat-
D
fat- ; Fat+
E
fat- ; Fat:Fat4
F
fat- ; Fat-ΔEGF
G
fat- ; Fat-ΔICD
H
tub-Wts; fat- Fat-ΔICD
I

Figure 9

Figure 10. Additional analysis of hair polarity phenotypes associated with Fat ICD motif mutations

A-I) Proximal anterior wings from $fat^{8}/fat^{G\text{-}rv}$ expressing A) *tub-Gal4 UAS-wts P[acman]V5:fatΔEGF[68A4],* B) *tub-Gal4 UAS-wts P[acman]V5:fatΔICD[68A4],* C) *P[acman]V5:fatP32[68A4]*, D) *P[acman]V5:fatΔA[68A4],* E) *P[acman]V5:fatΔC[68A4],* F) *P[acman]V5:fatΔE[68A4],* G) *P[acman]V5:fat-mI[68A4],* H) *P[acman]V5:fat-mIV[68A4],* I) *P[acman]V5:fat-mV[68A4]*. J-R) Abdomens from $fat^{8}/fat^{G\text{-}rv}$ expressing J) *P[acman]V5:fat[68A4],* K) *tub-Gal4 UAS-wts P[acman]V5:fatΔEGF[68A4],* L) *tub-Gal4 UAS-wts P[acman]V5:fatΔICD[68A4,* M) *P[acman]V5:fatΔA[68A4] ,* N) *P[acman]V5:fatΔC[68A4] ,* O) *P[acman]V5:fatΔE[68A4] ,* P) *P[acman]V5:fatΔD[68A4]/ P[acman]V5:fatΔF[68A4] ,* Q) *P[acman]V5:fat-mV[68A4] ,* R) *P[acman]V5:fatΔF[68A4]/P[acman]V5:fat:Fat4[68A4]*.

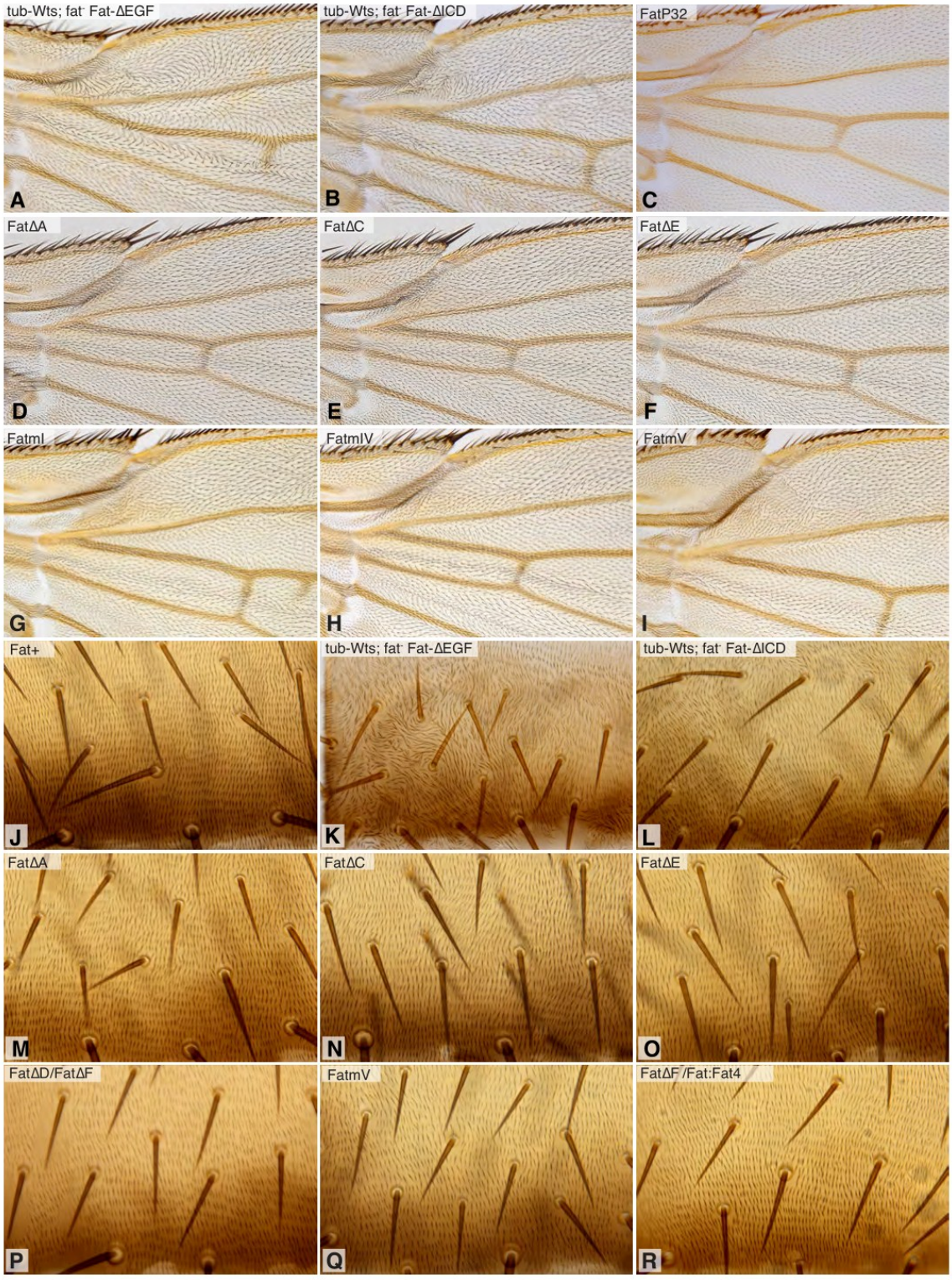
tub-Wts; fat- Fat-ΔEGF
A
tub-Wts; fat- Fat-ΔICD
B
FatP32
C
FatΔA
D
FatΔC
E
FatΔE
F
FatmI
G
FatmIV
H
FatmV
I
Fat+
J
tub-Wts; fat- Fat-ΔEGF
K
tub-Wts; fat- Fat-ΔICD
L
FatΔA
M
FatΔC
N
FatΔE
O
FatΔD/FatΔF
P
FatmV
Q
FatΔF/Fat:Fat4
R

Figure 10

Figure 11. Additional analysis of ridge polarity

Proximal anterior wings, visualized by cuticle refraction microscopy [91], from *fat*^{8}*/fat*$^{G\text{-}rv}$ expressing A) *P[acman]V5:fat[68A4],* D) *P[acman]V5:fatΔB[68A4],* E) *P[acman]V5:fatΔC[68A4],* F) *P[acman]V5:fatΔE[68A4],* G) *tub-Gal4 UAS-wts P[acman]V5:fatΔEGF[68A4],* H) *tub-Gal4 UAS-wts P[acman]V5:fat:Fat4[68A4], I) P[acman]V5:fat-mV[68A4],* or from *fat*$^{+}$ flies expressing *nub-Gal4* and B,C) *UAS-RNAi-ds*, J) *UAS-RNAi-dachs*, K) *UAS-RNAi-fat*, L) *UAS-Zyx:dachs*.

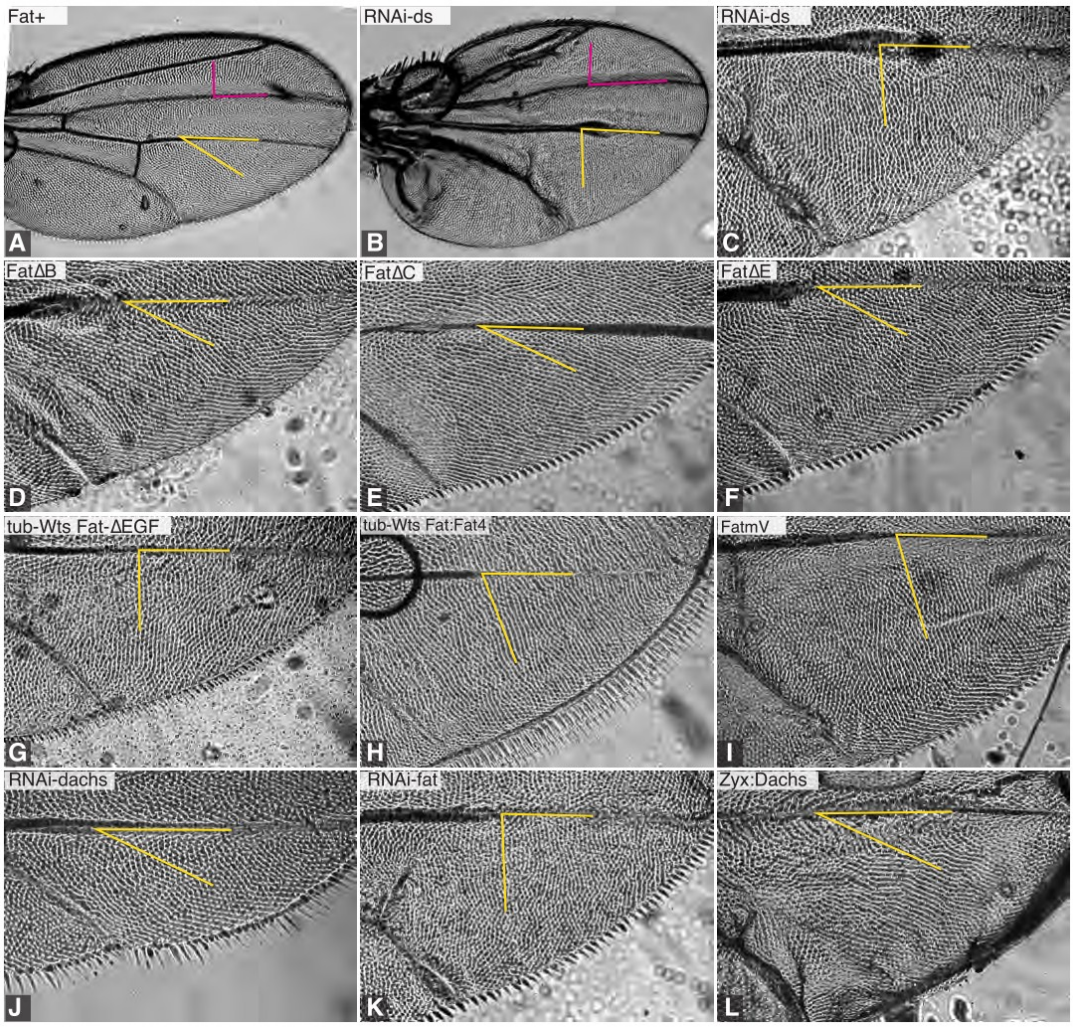

Figure 11

Figure 12. Additional analysis of Fat ICD phosphorylation

A) Western blots on S2 cell lysates expressing Fat-STI-4:FVH (STI-4) and point mutant derivatives, together with Dco or Dco^3, as indicated. The amino acids mutated in each construct are indicated in Supplementary Fig. S5. Of the mutants shown here, only P14 and P15 fail to exhibit the Dco-mediated mobility shift. B) The mobility shift induced by Ser to Asp mutations is not reversed by phosphatase treatment (CIP). C) Western blot on products of a kinase assay with vertebrate CKI shows that purified Fat-STI-4:FVH can be directly phosphorylated by CKI in vitro, with the extent of phosphorylation is proportional to the amount of enzyme; for comparison protein phosphorylated in vivo was run on the same gel. The S to A triple mutant Fat-STI-4-P32:FVH is still a substrate for CKI , but the degree of phosphorylation, as assayed by mobility shift, is reduced. D) Over-expression of *dco*^{3} in posterior cells, under *hh-Gal4* control (red), does not affect Dachs:Cit staining (green), Dachs:Cit in anterior cells serve as an internal control. Over-expression of Dco^3 mimics *dco*^{3} mutation; this confirms earlier studies of the lack of effect of *dco*^{3} mutant clones on Dachs localization [46].

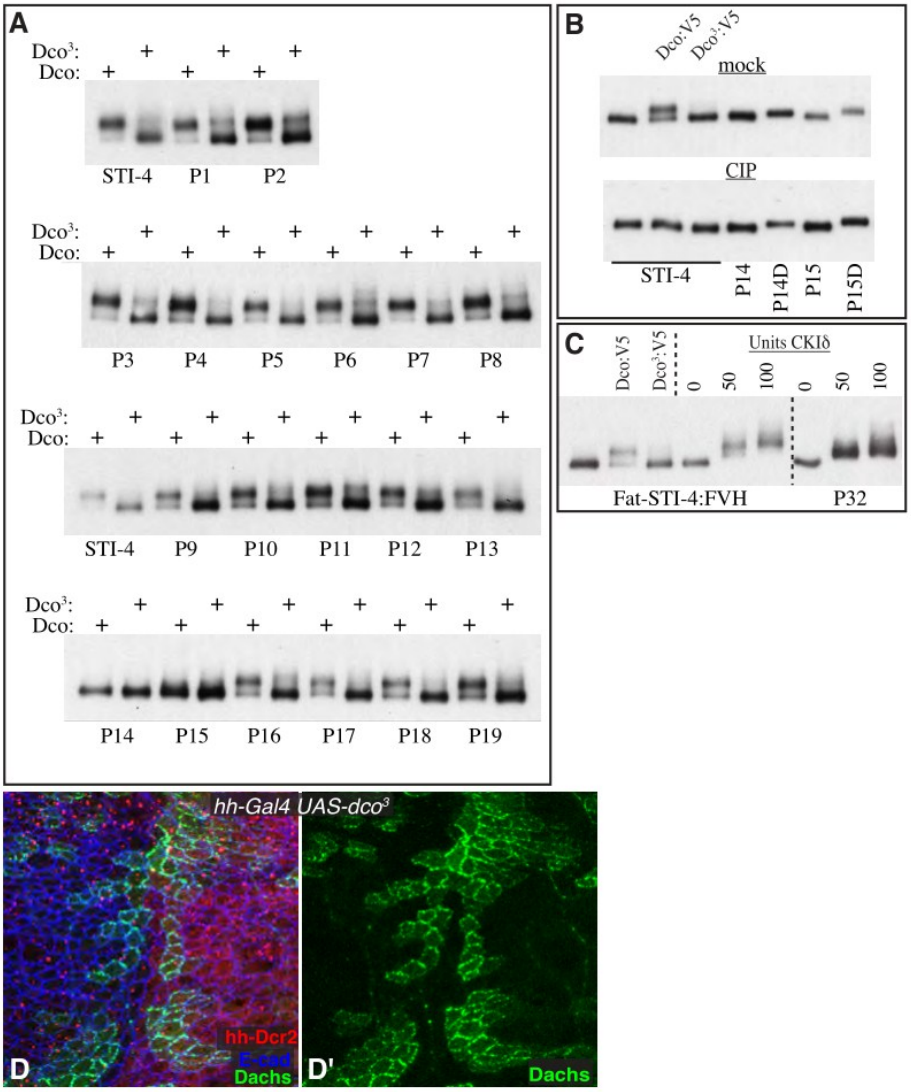
A
Dco3:
Dco:
STI-4 P1 P2
P3 P4 P5 P6 P7 P8
STI-4 P9 P10 P11 P12 P13
P14 P15 P16 P17 P18 P19
B
Dco:V5
Dco3:V5
mock
CIP
STI-4 P14 P14D P15 P15D
C
Dco:V5
Dco3:V5
Units CKIδ
0 50 100 0 50 100
Fat-STI-4:FVH P32
hh-Gal4 UAS-dco3
hh-Dcr2
E-cad
Dachs
D
D'
Dachs

Figure 12

Figure 13. Potential phosphorylation sites altered in point mutant constructs

Potential phosphorylation sites (Ser, Thr, or Tyr) within the Fat intracellular domain were mutated to Ala or Asp, as indicated, within a series of constructs, which were then analyzed for effects on Fat mobility or activity. First column indicates name of the construct, top row shows location of site within the intracellular domain, bottom row shows location within entire Fat coding sequence. Middle rows show amino acid mutations within each construct.

Location in whole Fat protein (5147aa)	mut V	mut IV	mut I	P33D	P33	P32D	P32	P27D	P26D	P25D	P31	P30	P29	P28	P27	P26	P25	P24	P23	P22	P21	P15D	P14D	P20	P19	P18	P17	P16	P15	P14	P13	P12	P11	P10	P9	P8	P7	P6	P5	P4	P3	P2	P1	Point mutants / Location in Fat intracellular domain (538 aa)
S 4781																																			A									S 172
S 4786																																			A									S 177
Y 4788																																			A									Y 179
T 4789																																			A									T 180
S 4796																																											A	S 187
S 4798																																											A	S 189
T 4808																																		A										T 199
T 4813																																		A										T 204
T 4825																																										A		T 216
S 4826																																										A		S 217
S 4828																																										A		S 219
T 4830																																										A		T 221
S 4833			A																														A											S 224
T 4834																																	A											T 225
S 4840			A																													A												S 231
S 4842			A																													A												S 233
S 4843			A																													A												S 234
S 4846			A																													A												S 237
S 4847			A																													A												S 238
T 4870																															A													T 261
T 4871																															A													T 262
S 4872																															A													S 263
S 4873																															A													S 264
S 4874																															A													S 265
S 4883																				A	A		D							A														S 274
S 4885				D	A														A		A		D							A														S 276
S 4888				D	A													A					D							A														S 279
S 4891						D	A			D							A				A		D							A														S 282
S 4895						D	A		D							A						D							A															S 286
S 4898						D	A	D							A							D							A															S 289
S 4901														A								D							A															S 292
S 4902													A									D							A															S 293
S 4903												A										D							A															S 294
S 4905											A											D							A															S 296
T 4919																												A																T 310
S 4920																												A																S 311
T 4924																																									A			T 315
S 4939		A																																						A				S 330
S 4942		A																																						A				S 333
T 4943																																								A				T 334
S 4948		A																																					A					S 339
S 4949		A																																					A					S 340
S 4950		A																																					A					S 341
S 4951		A																																					A					S 342
S 4957		A																									A																	S 348
S 4958		A																									A																	S 349
S 4959		A																									A																	S 350
S 4964		A																									A																	S 355
S 4973	A																																					A						S 364
S 4974	A																																					A						S 365
T 4975	A																																					A						T 366
S 4976	A																																					A						S 367
T 4977	A																																					A						T 368
S 4980	A																																											S 371
S 4984	A																																				A							S 375
T 4986																																					A							T 377
S 4988	A																																				A							S 379
Y 4992																																				A								Y 383
S 4996	A																									A																		S 387
S 4998	A																									A																		S 389
S 5004																									A																			S 395
T 5005																									A																			T 396
S 5006																									A																			S 397
S 5008																									A																			S 399
S 5014																								A																				S 405
S 5017																								A																				S 408
S 5021																								A																				S 412

CHAPTER IV

General Discussion

This dissertation first investigates the molecular mechanism of Zyx, a novel component of Fat-Hippo signaling, for signal transduction in Fat signaling. Then a structure-function analysis of Fat was conducted, to investigate how Fat coordinates distinctive pathways. The Fat-PCP activity is evolutionarily conserved from *Drosophila* to mammals, and a conserved four amino acid motif is found to be crucial for Fat-PCP. Hippo activity can be largely separated from PCP activity at the level of the Fat receptor, and phosphorylation is an essential factor in Fat-Hippo signaling transduction. Different Fat activity is correlated with distinctive Dachs localization profile, and directly manipulating Dachs localization could phenocopy loss of Fat activity. These results extend the knowledge of how Fat regulates growth and polarity through Dachs, and how Dachs interacts with Zyx to regulate Wts. Nevertheless, some questions rise from our observations. The mechanism of Dachs modifying Zyx is not clear, and how the downstream effector Wts is regulated by upstream signal inputs remains a mystery. It would be interesting to reveal possible regulating network of distinct Fat activity with other Hippo pathway components, for example, Scrib, which also has dual roles in polarity and growth.

Biochemical mechanism of Dachs promoting Wts/Zyx binding

Dachs, Zyx and Wts could bind one another, and Dachs could stimulate the binding between full length Zyx and Wts. These observations raise the possibility that Dachs/Zyx/Wts could form a triplex. However, since the amount of Zyx binding to Wts is much higher than that of Dachs (Chapter II, Figure 1H), it seems more plausible that Dachs works catalytically, or sequentially, to induce a conformational change of Zyx.

Dachs might interact directly or through recruiting other factors to make full-length Zyx be accessible to Wts.

One possibility to induce this conformational change might be phosphorylation of Zyx. In mammalian cells, full length Zyxin binds to LATS1 after being treated with kinase Cdc2 [56], which suggests a potentially conserved mechanism. However, in previous studies, no obvious mobility shift of over-expressing tagged Zyx in cultured S2 cells was observed, at the presence of Wts or Dachs. This might be due to that the mobility shift is too small for detection in regular protein gels. Further investigation might take advantage of Phos-tag gels and Calf Intestinal Alkaline Phosphatase treatment to examine if Zyx is phosphorylated [95].

Molecular mechanism of Wts regulated by Zyx/Dachs

Targeting Dachs to the membrane by fusing it with Zyx could reduce Wts protein level, which phenocopies *fat* mutants. The molecular mechanism of how Fat pathway regulating Wts abundance is not clear, and protein degradation system might be required. Recent studies show that both LATS1/2 could be ubiquitinated in cultured mammalian cells, and ITCH could be an E3 ligase for LATS1 [96]. One former post-doc in our lab, Xunlei Kang, had preliminary results showing that Wts protein could by ubiquitinated in S2 cells, and the stability of Wts could increase by blocking proteasome activity using MG132 treatment. At in vivo condition, preliminary experiments suggested that in *Drosophila* imaginal discs, MG132 treatment could suppress the reduction of Wts level caused by dco^{3} mutation. These results indicate that ubiquitin-proteasome system might be involved in regulating Wts level.

One major step investigating protein degradation mechanism is to identify the E3 ligase(s) for Wts. ITCH, along with the *Drosophila melanogaster* ortholog Suppressor of deltex (Su(dx)), belongs to the Nedd4 family of HECT E3 ubiquitin ligases [97]. *Drosophila* Nedd4 family has three members: dNedd4 (neuronal precursor cell expressed developmentally down regulated 4), Su(dx) (ITCH or AIP4) and SMURF (Smad ubiquitination regulatory factor) [97]. dNedd4 mediates the endocytosis of Comm [98], and regulates degradation of Notch and Deltex. Su(dx) is also a negative regulator of Notch signaling through affecting Notch ubiquitination [99]. SMURF is a negative regulator of decapentaplegic (Dpp) signaling.

Over-expression of Su(dx) induces overgrowth in wing discs, suggesting it to be a positive regulator of growth [100]. Preliminary experiments show that in a western blot of 3rd instar discs, knock-down of Su(dx) or Smurf by RNAi could increase the abundance of the faster mobility Wts isoform, without obviously jeopardizing the slower mobility isoform, suggesting the faster-moving Wts band might be more sensitive to protein degradation (Figure 2 lane 4, 5 & 8). However, to our surprise, knocking down Su(dx) and Smurf in wing discs doesn't affect overgrowth or reporters of Fat-Hpo signaling activity, such as expanded (ex) expression (ex-lacZ) and th expression (th-lacZ, Diap1). Su(dx) RNAi also could not suppress the *fat* RNAi phenotype. We suspect the lack of loss-of-function phenotype might due to redundancy among the 3 Nedd4 family proteins.

Besides from affecting Wts levels, Fat pathway might regulate Wts post-translational modification. When the protein gels were run for extended time, the band representing Wts would run as doublet and *fat* mutants could affect the mobility shift of this doublet,

in western blot of 3rd instar wing discs lysates. In wild-type control flies, most of Wts protein is in one single band, while there is trace of a lower band which is not distinguishable from background; when Fat is knocked down by RNAi, the abundance of upper band decreases dramatically, while the lower band become predominant (Figure 1 lane 1&2). Consisted with the notion that Dachs and Zyx are genetically required for Fat to regulate Wts protein levels, Zyx RNAi or Dachs mutant could suppress this effect on mobility, rendering *fat dach*s double mutant or Fat Zyx double RNAi behaves similarly to OR (Figure 1 lane 3&6) Importantly, *ex* mutant doesn't have effect on Wts mobility, suggesting the mobility shift is specific for Fat branch of Fat-Hpo signaling (Figure 1 lane 7). Another intriguing phenomenon is that an antimorphic dco^3 mutant and overexpression of a fusion protein of Zyx and dachs induce further decrease of the Wts lower band (Figure 1 lane 8&4).

The significance and mechanism responsible for this mobility change are unknown. The faster mobility isoform of Wts might represent a fragment of Wts, which is cleaved from the slower mobility isoform when *fat* is knocked-down. Alternatively, the two different mobility isoforms of Wts may represent a phosphorylated and unphosphorylated form. Since full length Wts is a relatively large protein with molecular weight of 120kD, the big mobility difference observed can't be explained unless it is magnified by a phosphorylation induced conformation change.

We identified a correlation between Dachs localization and Fat signaling, and proved that altered Dachs localization could transduce Fat signaling. It's not clear if Dachs localization is also associated with different Wts level or mobility. And the hair phenotype of Wts-rescued *fat* mutants appear to us similar to that described for *fat*

mutants rescued by the Fat ICD-only expressing construct fatICD, which has been interpreted as a partial rescue of hair polarity [93]. Therefore, some of the hair PCP phenotype ascribed to *fat* could reflect effects on transcription of downstream target genes, mediated via Wts. It would be interesting to examine how different Fat activities and Dachs localizations are associated with level or post-translational modification of Wts.

Scrib might interact with Fat 'F' motif

The Drosophila tumor suppressor protein Scrib is required for epithelial polarity, neuroblast polarity, neuroblast spindle asymmetry and limiting cell proliferation [101]. Recent studies placed Scrib in the Hippo pathway network; Ft requires Scrib to interact with Ex and Dachs, and for regulating Wts levels and stability [102]. One interesting feature of Scrib is the four PDZ domains. The four amino acids in "F" motif resemble a PDZ domain binding motif, which suggests that it might interact with a PDZ domain-containing protein, presumably, Scrib. Investigation the interaction between Fat and Scrib might provide clues how different inputs to Hippo pathway are coordinated.

Figures

Figure 1. Post-translational modification of Wts

Western blot on lysates of 3rd instar wing discs from *tubGal80ts tubGal4 UAS-dcr2/OR* (control), *tubGal80ts tubGal4 UAS-dcr2/UAS-RNAi-fat, tubGal80ts tubGal4 UAS-dcr2/ UAS-RNAi-fat UAS-RNAi-Zyx, tubGal80ts tubGal4 UAS-dcr2/ UAS-Zyx-Dachs fusion, tubGal4 UAS-dcr2/ UAS-Zyx:V5, $fat^{8/G\text{-}rV}$ $dachs^{GC13/GC13}$, $ex^{e1/e1}$, $dco^{3/3}$, OR,* probed with anti-Wts and anti-GAPDH antisera, as indicated. Similar amounts of total protein were loaded in each lane.

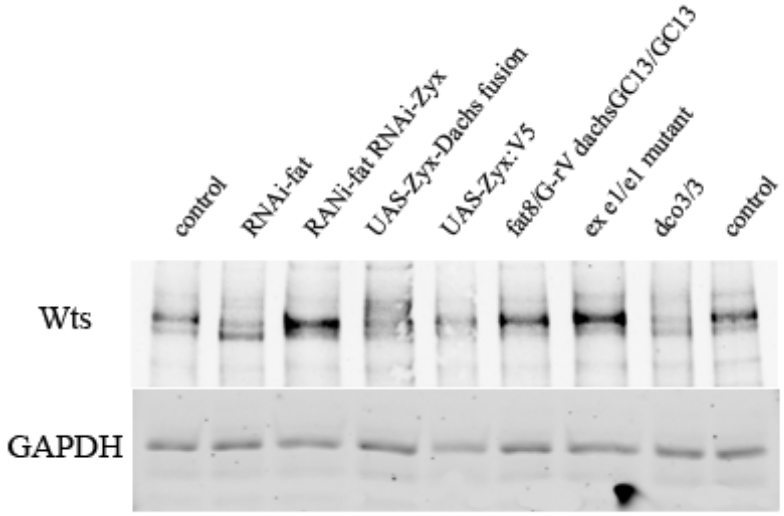

Figure 2. Nedd4 family members could affect Wts post-translational modification. Western blot on lysates of 3rd instar wing discs from *tubGal80ts tubGal4 UAS-dcr2/OR* (control), *tubGal80ts tubGal4 UAS-dcr2/UAS-RNAi-fat, tubGal80ts tubGal4 UAS-dcr2/ UAS-Su(dx), tubGal80ts tubGal4 UAS-dcr2/ UAS-RNAi-Su(dx) 48h, tubGal80ts tubGal4 UAS-dcr2/ UAS-RNAi-Su(dx) 72h, Su(dx)$^{sp/32}$, Su(dx)$^{sp/sp}$, tubGal80ts tubGal4 UAS-dcr2/ UAS-RNAi-Smurf*, probed with anti-Wts and anti-GAPDH antisera, as indicated. Similar amounts of total protein were loaded in each lane.

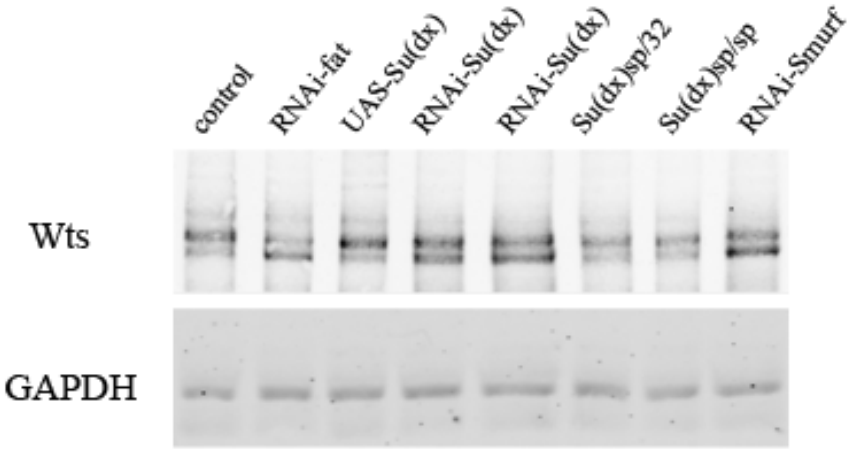

Reference

1. Wartlick, O., et al., *Understanding morphogenetic growth control -- lessons from flies.* Nat Rev Mol Cell Biol, 2011. **12**(9): p. 594-604.
2. McClure, K.D. and G. Schubiger, *Transdetermination: Drosophila imaginal disc cells exhibit stem cell-like potency.* Int J Biochem Cell Biol, 2007. **39**(6): p. 1105-18.
3. Whittle, J.R., *Pattern formation in imaginal discs.* Semin Cell Biol, 1990. **1**(3): p. 241-52.
4. Zhao, B., et al., *The Hippo-YAP pathway in organ size control and tumorigenesis: an updated version.* Genes Dev, 2010. **24**(9): p. 862-74.
5. Staley, B.K. and K.D. Irvine, *Warts and Yorkie mediate intestinal regeneration by influencing stem cell proliferation.* Curr Biol, 2010. **20**(17): p. 1580-7.
6. Reddy, B.V., C. Rauskolb, and K.D. Irvine, *Influence of fat-hippo and notch signaling on the proliferation and differentiation of Drosophila optic neuroepithelia.* Development, 2010. **137**(14): p. 2397-408.
7. Harvey, K.F. and I.K. Hariharan, *The hippo pathway.* Cold Spring Harb Perspect Biol, 2012. **4**(8): p. a011288.
8. Pan, D., *The hippo signaling pathway in development and cancer.* Dev Cell, 2010. **19**(4): p. 491-505.
9. Halder, G. and R.L. Johnson, *Hippo signaling: growth control and beyond.* Development, 2011. **138**(1): p. 9-22.
10. Harvey, K. and N. Tapon, *The Salvador-Warts-Hippo pathway - an emerging tumour-suppressor network.* Nat Rev Cancer, 2007. **7**(3): p. 182-91.
11. Glantschnig, H., G.A. Rodan, and A.A. Reszka, *Mapping of MST1 kinase sites of phosphorylation. Activation and autophosphorylation.* J Biol Chem, 2002. **277**(45): p. 42987-96.
12. Lee, K.K. and S. Yonehara, *Phosphorylation and dimerization regulate nucleocytoplasmic shuttling of mammalian STE20-like kinase (MST).* J Biol Chem, 2002. **277**(14): p. 12351-8.
13. Wei, X., T. Shimizu, and Z.C. Lai, *Mob as tumor suppressor is activated by Hippo kinase for growth inhibition in Drosophila.* EMBO J, 2007. **26**(7): p. 1772-81.
14. Wu, S., et al., *hippo encodes a Ste-20 family protein kinase that restricts cell proliferation and promotes apoptosis in conjunction with salvador and warts.* Cell, 2003. **114**(4): p. 445-56.
15. Lai, Z.C., et al., *Control of cell proliferation and apoptosis by mob as tumor suppressor, mats.* Cell, 2005. **120**(5): p. 675-85.
16. Edgar, B.A., *From cell structure to transcription: Hippo forges a new path.* Cell, 2006. **124**(2): p. 267-73.
17. Thompson, B.J. and S.M. Cohen, *The Hippo pathway regulates the bantam microRNA to control cell proliferation and apoptosis in Drosophila.* Cell, 2006. **126**(4): p. 767-74.
18. Irvine, K.D., *Integration of intercellular signaling through the Hippo pathway.* Semin Cell Dev Biol, 2012. **23**(7): p. 812-7.

19. Baumgartner, R., et al., *The WW domain protein Kibra acts upstream of Hippo in Drosophila.* Dev Cell, 2010. **18**(2): p. 309-16.
20. Sun, G. and K.D. Irvine, *Regulation of Hippo signaling by Jun kinase signaling during compensatory cell proliferation and regeneration, and in neoplastic tumors.* Dev Biol, 2011. **350**(1): p. 139-51.
21. Cho, E., et al., *Delineation of a Fat tumor suppressor pathway.* Nat Genet, 2006. **38**(10): p. 1142-50.
22. Thomas, C. and D. Strutt, *The roles of the cadherins Fat and Dachsous in planar polarity specification in Drosophila.* Dev Dyn, 2012. **241**(1): p. 27-39.
23. Goodrich, L.V. and D. Strutt, *Principles of planar polarity in animal development.* Development, 2011. **138**(10): p. 1877-92.
24. Simons, M. and M. Mlodzik, *Planar cell polarity signaling: from fly development to human disease.* Annu Rev Genet, 2008. **42**: p. 517-40.
25. Wong, L.L. and P.N. Adler, *Tissue polarity genes of Drosophila regulate the subcellular location for prehair initiation in pupal wing cells.* J Cell Biol, 1993. **123**(1): p. 209-21.
26. Doyle, K., et al., *The Frizzled Planar Cell Polarity signaling pathway controls Drosophila wing topography.* Dev Biol, 2008. **317**(1): p. 354-67.
27. Baena-Lopez, L.A., I. Rodriguez, and A. Baonza, *The tumor suppressor genes dachsous and fat modulate different signalling pathways by regulating dally and dally-like.* Proc Natl Acad Sci U S A, 2008. **105**(28): p. 9645-50.
28. Mao, Y., et al., *Planar polarization of the atypical myosin Dachs orients cell divisions in Drosophila.* Genes Dev, 2011. **25**(2): p. 131-6.
29. Reddy, B.V. and K.D. Irvine, *The Fat and Warts signaling pathways: new insights into their regulation, mechanism and conservation.* Development, 2008. **135**(17): p. 2827-38.
30. Tanoue, T. and M. Takeichi, *New insights into Fat cadherins.* J Cell Sci, 2005. **118**(Pt 11): p. 2347-53.
31. Saburi, S., et al., *Loss of Fat4 disrupts PCP signaling and oriented cell division and leads to cystic kidney disease.* Nat Genet, 2008. **40**(8): p. 1010-5.
32. Sopko, R. and H. McNeill, *The skinny on Fat: an enormous cadherin that regulates cell adhesion, tissue growth, and planar cell polarity.* Curr Opin Cell Biol, 2009. **21**(5): p. 717-23.
33. Ishikawa, H.O., et al., *Four-jointed is a Golgi kinase that phosphorylates a subset of cadherin domains.* Science, 2008. **321**(5887): p. 401-4.
34. Brittle, A.L., et al., *Four-jointed modulates growth and planar polarity by reducing the affinity of dachsous for fat.* Curr Biol, 2010. **20**(9): p. 803-10.
35. Simon, M.A., et al., *Modulation of fat:dachsous binding by the cadherin domain kinase four-jointed.* Curr Biol, 2010. **20**(9): p. 811-7.
36. Rogulja, D., C. Rauskolb, and K.D. Irvine, *Morphogen control of wing growth through the Fat signaling pathway.* Dev Cell, 2008. **15**(2): p. 309-21.
37. Willecke, M., et al., *Boundaries of Dachsous Cadherin activity modulate the Hippo signaling pathway to induce cell proliferation.* Proc Natl Acad Sci U S A, 2008. **105**(39): p. 14897-902.

38. Mao, Y., et al., *Dachs: an unconventional myosin that functions downstream of Fat to regulate growth, affinity and gene expression in Drosophila.* Development, 2006. **133**(13): p. 2539-51.
39. Ambegaonkar, A.A., et al., *Propagation of Dachsous-Fat planar cell polarity.* Curr Biol, 2012. **22**(14): p. 1302-8.
40. Bosveld, F., et al., *Mechanical control of morphogenesis by Fat/Dachsous/Four-jointed planar cell polarity pathway.* Science, 2012. **336**(6082): p. 724-7.
41. Zilian, O., et al., *double-time is identical to discs overgrown, which is required for cell survival, proliferation and growth arrest in Drosophila imaginal discs.* Development, 1999. **126**(23): p. 5409-20.
42. Price, M.A., *CKI, there's more than one: casein kinase I family members in Wnt and Hedgehog signaling.* Genes Dev, 2006. **20**(4): p. 399-410.
43. Strutt, H., M.A. Price, and D. Strutt, *Planar polarity is positively regulated by casein kinase Iepsilon in Drosophila.* Curr Biol, 2006. **16**(13): p. 1329-36.
44. Klein, T.J., et al., *CKIepsilon/discs overgrown promotes both Wnt-Fz/beta-catenin and Fz/PCP signaling in Drosophila.* Curr Biol, 2006. **16**(13): p. 1337-43.
45. Guan, J., et al., *The Drosophila casein kinase Iepsilon/delta Discs overgrown promotes cell survival via activation of DIAP1 expression.* Dev Biol, 2007. **303**(1): p. 16-28.
46. Feng, Y. and K.D. Irvine, *Processing and phosphorylation of the Fat receptor.* Proc Natl Acad Sci U S A, 2009. **106**(29): p. 11989-94.
47. Sopko, R., et al., *Phosphorylation of the tumor suppressor fat is regulated by its ligand Dachsous and the kinase discs overgrown.* Curr Biol, 2009. **19**(13): p. 1112-7.
48. Das Thakur, M., et al., *Ajuba LIM proteins are negative regulators of the Hippo signaling pathway.* Curr Biol, 2010. **20**(7): p. 657-62.
49. Renfranz, P.J., et al., *Molecular and phylogenetic characterization of Zyx102, a Drosophila orthologue of the zyxin family that interacts with Drosophila Enabled.* Gene, 2003. **305**(1): p. 13-26.
50. Kadrmas, J.L. and M.C. Beckerle, *The LIM domain: from the cytoskeleton to the nucleus.* Nat Rev Mol Cell Biol, 2004. **5**(11): p. 920-31.
51. Drees, B., et al., *Characterization of the interaction between zyxin and members of the Ena/vasodilator-stimulated phosphoprotein family of proteins.* J Biol Chem, 2000. **275**(29): p. 22503-11.
52. Nix, D.A., et al., *Targeting of zyxin to sites of actin membrane interaction and to the nucleus.* J Biol Chem, 2001. **276**(37): p. 34759-67.
53. Nix, D.A. and M.C. Beckerle, *Nuclear-cytoplasmic shuttling of the focal contact protein, zyxin: a potential mechanism for communication between sites of cell adhesion and the nucleus.* J Cell Biol, 1997. **138**(5): p. 1139-47.
54. Kanungo, J., et al., *Ajuba, a cytosolic LIM protein, shuttles into the nucleus and affects embryonal cell proliferation and fate decisions.* Mol Biol Cell, 2000. **11**(10): p. 3299-313.
55. Huggins, C.J. and I.L. Andrulis, *Cell cycle regulated phosphorylation of LIMD1 in cell lines and expression in human breast cancers.* Cancer Lett, 2008. **267**(1): p. 55-66.

56. Hirota, T., et al., *Zyxin, a regulator of actin filament assembly, targets the mitotic apparatus by interacting with h-warts/LATS1 tumor suppressor.* J Cell Biol, 2000. **149**(5): p. 1073-86.
57. Hirota, T., et al., *Aurora-A and an interacting activator, the LIM protein Ajuba, are required for mitotic commitment in human cells.* Cell, 2003. **114**(5): p. 585-98.
58. Cattaruzza, M., C. Lattrich, and M. Hecker, *Focal adhesion protein zyxin is a mechanosensitive modulator of gene expression in vascular smooth muscle cells.* Hypertension, 2004. **43**(4): p. 726-30.
59. Hou, Z., et al., *LIM protein Ajuba functions as a nuclear receptor corepressor and negatively regulates retinoic acid signaling.* Proc Natl Acad Sci U S A, 2010. **107**(7): p. 2938-43.
60. Rauskolb, C., et al., *Zyxin links fat signaling to the hippo pathway.* PLoS Biol, 2011. **9**(6): p. e1000624.
61. Vervenne, H.B., et al., *Targeted disruption of the mouse Lipoma Preferred Partner gene.* Biochem Biophys Res Commun, 2009. **379**(2): p. 368-73.
62. Hoffman, L.M., et al., *Targeted disruption of the murine zyxin gene.* Mol Cell Biol, 2003. **23**(1): p. 70-9.
63. Grunewald, T.G., S.M. Pasedag, and E. Butt, *Cell Adhesion and Transcriptional Activity - Defining the Role of the Novel Protooncogene LPP.* Transl Oncol, 2009. **2**(3): p. 107-16.
64. Abe, Y., et al., *LATS2-Ajuba complex regulates gamma-tubulin recruitment to centrosomes and spindle organization during mitosis.* FEBS Lett, 2006. **580**(3): p. 782-8.
65. Hirata, H., H. Tatsumi, and M. Sokabe, *Zyxin emerges as a key player in the mechanotransduction at cell adhesive structures.* Commun Integr Biol, 2008. **1**(2): p. 192-195.
66. Beckerle, M.C., *Zyxin: zinc fingers at sites of cell adhesion.* Bioessays, 1997. **19**(11): p. 949-57.
67. Woolner, S. and W.M. Bement, *Unconventional myosins acting unconventionally.* Trends in Cell Biology, 2009. **19**(6): p. 245-52.
68. Shraiman, B.I., *Mechanical feedback as a possible regulator of tissue growth.* Proc Natl Acad Sci USA, 2005. **102**(9): p. 3318-23.
69. Aegerter-Wilmsen, T., et al., *Model for the regulation of size in the wing imaginal disc of Drosophila.* Mech Dev, 2007. **124**(4): p. 318-26.
70. Ishikawa, H.O., et al., *Four-jointed is a Golgi kinase that phosphorylates a subset of cadherin domains.* Science, 2008. **321**: p. 401-404.
71. Thomas, C. and D. Strutt, *The roles of the cadherins Fat and Dachsous in planar polarity specification in Drosophila.* Developmental dynamics, 2011. **241**: p. 27-39.
72. Staley, B.K. and K.D. Irvine, *Hippo signaling in Drosophila: recent advances and insights.* Dev Dyn, 2012. **241**(1): p. 3-15.
73. Cho, E. and K.D. Irvine, *Action of fat, four-jointed, dachsous and dachs in distal-to-proximal wing signaling.* Development, 2004. **131**(18): p. 4489-500.
74. Brittle, A., C. Thomas, and D. Strutt, *Planar Polarity Specification through Asymmetric Subcellular Localization of Fat and Dachsous.* Current biology, 2012. **22**: p. 907-914.

75. Bosveld, F., et al., *Mechanical Control of Morphogenesis by Fat/Dachsous/Four-Jointed Planar Cell Polarity Pathway.* Science, 2012. **336**: p. 724-727.
76. Ambegaonkar, A.A., et al., *Propagation of Dachsous-Fat Planar Cell Polarity.* Current Biology, 2012. **22**: p. 1302-1308.
77. Mao, Y., et al., *Planar polarization of the atypical myosin Dachs orients cell divisions in Drosophila.* Genes & Development, 2011. **25**(2): p. 131-136.
78. Fanto, M., et al., *The tumor-suppressor and cell adhesion molecule Fat controls planar polarity via physical interactions with Atrophin, a transcriptional co-repressor.* Development, 2003. **130**(4): p. 763-74.
79. Li, W., A. Kale, and N.E. Baker, *Oriented cell division as a response to cell death and cell competition.* Current biology, 2009. **19**(21): p. 1821-1826.
80. Van Hateren, N.J., et al., *FatJ acts via the Hippo mediator Yap1 to restrict the size of neural progenitor cell pools.* Development, 2011. **138**(10): p. 1893-902.
81. Mao, Y., et al., *Characterization of a Dchs1 mutant mouse reveals requirements for Dchs1-Fat4 signaling during mammalian development.* Development, 2011. **138**(5): p. 947-57.
82. Warming, S., et al., *Simple and highly efficient BAC recombineering using galK selection.* Nucleic Acids Res, 2005. **33**(4): p. e36.
83. Venken, K.J., et al., *P[acman]: a BAC transgenic platform for targeted insertion of large DNA fragments in D. melanogaster.* Science, 2006. **314**(5806): p. 1747-51.
84. Groth, A.C., et al., *Construction of transgenic Drosophila by using the site-specific integrase from phage phiC31.* Genetics, 2004. **166**(4): p. 1775-82.
85. McNeill, H., *Planar cell polarity and the kidney.* J Am Soc Nephrol, 2009. **20**(10): p. 2104-11.
86. Feng, Y. and K.D. Irvine, *Fat and expanded act in parallel to regulate growth through warts.* Proc Natl Acad Sci U S A, 2007. **104**(51): p. 20362-7.
87. Matakatsu, H. and S.S. Blair, *Separating the adhesive and signaling functions of the Fat and Dachsous protocadherins.* Development, 2006. **133**(12): p. 2315-24.
88. Aigouy, B., et al., *Cell flow reorients the axis of planar polarity in the wing epithelium of Drosophila.* Cell, 2010. **142**(5): p. 773-786.
89. Baena-Lopez, L.A., A. Baonza, and A. Garcia-Bellido, *The orientation of cell divisions determines the shape of Drosophila organs.* Curr Biol, 2005. **15**(18): p. 1640-4.
90. Hogan, J., et al., *Two frizzled planar cell polarity signals in the Drosophila wing are differentially organized by the Fat/Dachsous pathway.* PLoS genetics, 2011. **7**(2): p. e1001305.
91. Doyle, K., et al., *The Frizzled Planar Cell Polarity signaling pathway controls Drosophila wing topography.* Developmental Biology, 2008. **317**(1): p. 354-367.
92. Casal, J., P.A. Lawrence, and G. Struhl, *Two separate molecular systems, Dachsous/Fat and Starry night/Frizzled, act independently to confer planar cell polarity.* Development, 2006. **133**(22): p. 4561-72.
93. Matakatsu, H. and S.S. Blair, *Separating planar cell polarity and Hippo pathway activities of the protocadherins Fat and Dachsous.* Development, 2012. **139**(8): p. 1498-508.

94. Casal, J., P.A. Lawrence, and G. Struhl, *Two separate molecular systems, Dachsous/Fat and Starry night/Frizzled, act independently to confer planar cell polarity.* Development, 2006. **133**(22): p. 4561-4572.
95. Oh, H., B.V. Reddy, and K.D. Irvine, *Phosphorylation-independent repression of Yorkie in Fat-Hippo signaling.* Dev Biol, 2009. **335**(1): p. 188-97.
96. Salah, Z., G. Melino, and R.I. Aqeilan, *Negative regulation of the Hippo pathway by E3 ubiquitin ligase ITCH is sufficient to promote tumorigenicity.* Cancer Res, 2011. **71**(5): p. 2010-20.
97. Rotin, D. and S. Kumar, *Physiological functions of the HECT family of ubiquitin ligases.* Nat Rev Mol Cell Biol, 2009. **10**(6): p. 398-409.
98. Ing, B., et al., *Regulation of Commissureless by the ubiquitin ligase DNedd4 is required for neuromuscular synaptogenesis in Drosophila melanogaster.* Mol Cell Biol, 2007. **27**(2): p. 481-96.
99. Qiu, L., et al., *Recognition and ubiquitination of Notch by Itch, a hect-type E3 ubiquitin ligase.* J Biol Chem, 2000. **275**(46): p. 35734-7.
100. Mazaleyrat, S.L., et al., *Down-regulation of Notch target gene expression by Suppressor of deltex.* Dev Biol, 2003. **255**(2): p. 363-72.
101. Albertson, R., et al., *Scribble protein domain mapping reveals a multistep localization mechanism and domains necessary for establishing cortical polarity.* J Cell Sci, 2004. **117**(Pt 25): p. 6061-70.
102. Verghese, S., et al., *Scribble acts in the Drosophila fat-hippo pathway to regulate warts activity.* PLoS One, 2012. **7**(11): p. e47173.

CURRICULUM VITAE

GUOHUI PAN

EDUCATION:

Rutgers, the State University of New Jersey, New Brunswick, NJ
Ph.D., The Joint Graduate Program in Neuroscience (2013)

University of Medicine & Dentistry of New Jersey, Piscataway, NJ
Ph.D. candidate, The Joint Graduate Program in Neuroscience (2007-2008)

Tsinghua University, Beijing, China
Bachelor of Science, Department of Biological Science and Biotechnology (2005)

PUBLICATION:

[1] Pan, G., Feng, Y., Ambegaonkar, A. A., Sun, G., Huff M., Rauskolb, C. and Irvine, K. D. (2013). Signal transduction by the Fat cytoplasmic domain. Development. 2013 Feb;140(4):831-42.

[2] Ambegaonkar, A. A., Pan, G., Mani, M., Feng, Y. and Irvine, K. D. (2012). Propagation of Dachsous-Fat Planar Cell Polarity. Current Biology 22, 1302-1308.

[3] Rauskolb, C., Pan, G., Reddy, B. V., Oh, H. and Irvine, K. D. (2011). Zyxin links fat signaling to the hippo pathway. PLoS biology 9, e1000624.

[4] Qian M, Pan G, Sun L, Feng C, Xie Z, Tully T, Zhong Y. Receptor-like tyrosine phosphatase PTP10D is required for long-term memory in Drosophila. The Journal of Neuroscience. 2007 Apr 18; 27 (16): 4396-402. (*Qian and Pan contribute equally).